Interbacterial AI-2 communication drives stage-specific genetic programs to support *Salmonella* colonisation in the murine gut

Anmol Singh[a], Abhilash Vijay Nair[a,d], R. S. Rajmani[c], Dipshikha Chakravortty[a,c]*

[a]Department of Microbiology and Cell Biology, Division of Biological

[b]Molecular Biophysics Unit, Indian Institute of Science, Bengaluru, India

[c]Adjunct Faculty, School of Biology, Indian Institute of Science Education and Research, Thiruvananthapuram, India

[d]Present address: Department of Microbiology and Immunology, Vagelos College of Physicians and Surgeons, Columbia University, New York, NY 10032, USA

*Corresponding author: dipa@iisc.ac.in,

Tel: +91 80 2293 2842,

Fax: +91 80 2360 2697

Abstract

The cooperative response through AI-2 allows *Salmonella* to coordinate and regulate its community behaviours crucial for its survival and infection. Understanding these mechanisms is essential for developing strategies to interfere with *Salmonella's* ability to cause disease. In this study, we report that *Salmonella* Typhimurium uses AI-2 signaling to modulate the expression of chemotaxis and motility-associated genes and the formation of flagella on the bacterial cell surface. The AI-2 acts as a chemoattractant, and the cascade mediates the chemotactic response of *Salmonella.* Such regulations assist in the attachment and invasion of *Salmonella* into intestinal epithelial cells both *in vitro* and *in a* murine model. Furthermore, we determined that HilD, known to regulate motility by induction of a chemoreceptor and SPI-1 in *Salmonella*, along with key SPI-1 genes, is underexpressed in the absence of LuxS/AI-2 signaling, which unravels a complex regulatory network by AI-2 in *Salmonella*. Beyond the initial phase, this signaling facilitates survival in the presence of polymyxin B and supports intracellular survival and persistence within epithelial cells by regulating the *pmrD/AB* system, thereby evading the antimicrobial peptide immune response. Additionally, our findings show that *Salmonella* activates its LuxS/AI-2 signalling cascade within the Caco-2 epithelial cells. Complimentary observation through transcriptomic profiling revealed that LuxS/AI-2 signalling governs the coordinated regulation of genes implicated in distinct phases of *Salmonella* pathogenesis. Lastly using a mouse model, we show that AI-2 signaling is critical

36 for organ colonization and virulence of *Salmonella,* and inhibition of LuxS/AI-2
37 signaling in combination with antibiotics can be an alternative therapeutic
38 approach. Thus, our study dissects an integrated regulatory mechanism by which
39 AI-2 signaling mediates critical processes during multiple stages of *Salmonella*
40 Typhimurium pathogenesis.

41

42 **Introduction**

43 Bacteria were initially thought to be solitary microbes that led an independent life
44 cycle of multiplying and increasing their numbers, and some of them could cause
45 life-threatening infections. However, a series of discoveries led to unravelling the
46 mode of communication in these little beings referred to as quorum sensing (1-
47 3). This process involves the production and secretion of chemical signals that
48 are sensed by the neighbouring cells in the bacterial community and orchestrate
49 a myriad of genes and pathways, resulting in coordinated behaviours such as
50 adaptation, virulence and other critical community behaviours underscoring the
51 advantages of communal living among bacterial populations (4, 5). Bacterial
52 pathogenesis is very well governed by this communication paradigm. The
53 pathogen, upon entry into the host, has to decide to stay and colonise, or utilise
54 the host nutrients and run or employ all its virulence strategies without worrying
55 about the repercussions. Interestingly, the community communicates, coordinates
56 and makes the decision on the microbial pathogenesis (6, 7). Bacterial pathogens
57 are the sole cause of serious bacterial infections (SBIs) worldwide, with an
58 estimated 7.7 million deaths globally, with a rise in antimicrobial resistance,
59 which further worsens the situation(8). *Salmonella* enterica serovar Typhimurium
60 (STM) is a prominent etiological agent of foodborne illnesses and a leading
61 contributor to non-typhoidal salmonellosis (NTS)(9). It faces very long odds
62 while seeking to colonise and breach the intestinal barrier, including acidic pH,
63 limited nutrient availability, bile salt toxicity, and competition from gut

64 microbiota. It is critical for the bacteria to establish and increase in number,
65 reaching the infectious dose to invade the host epithelial cells. Upon breaching
66 the epithelial barrier, it is engulfed by macrophages in the lamina propria,
67 facilitating its systemic dissemination throughout the host (10-13). With the
68 fluctuations of extreme conditions, *Salmonella* needs to be adept at sensing,
69 responding, and adapting to unprecedented situations.

70 *Salmonella* uses the autoinducer-2 (AI-2) chemical messenger for their
71 communication. This intercellular communication, called quorum sensing,
72 enables *Salmonella* to regulate and synchronize their behaviors when present at
73 high cell densities(14-16). The AI-2 in *S*. Typhimurium is a byproduct of the
74 activated methyl cycle (AMC), where initially, the S-adenosyl methionine(SAM)
75 is converted into S-adenosylhomocysteine(SAH) by methyl transferases (17).
76 The SAH is subsequently converted to the precursor of AI-2 molecule 4,5
77 dihydroxy-2,3-pentanedione (DPD) by the enzymes Pfs and LuxS,
78 respectively(18). Finally, DPD molecules autocyclize into (2R,4S)-2-methyl-
79 2,3,3,4-tetrahydroxytetra-hydrofuran (AI-2) molecules(19, 20).

80 Although the LuxS/AI-2 quorum-sensing signaling pathway is well
81 characterized, its physiological significance remains only partially understood in
82 *Salmonella* pathogenesis despite being a thoroughly established system. Studies
83 suggest that *Salmonella* quorum sensing regulates virulence, biofilm formation,
84 motility, and antimicrobial resistance by regulating *Salmonella* Pathogenicity

85 Island-1, flagella, and antioxidative genes(21-23). Further, there is evidence of
86 involvement of AI-2 in motility and chemotaxis in the Ag43-dependent
87 aggregation of *E. coli* and its roles in *E. coli* gut colonization(24). The study also
88 shows that chemotaxis towards self-produced AI-2 provides *E. coli* a fitness
89 advantage during gut colonization, hinges on fructoselysine metabolism(25). AI-
90 2, a molecule produced and detected by numerous bacterial species, has also been
91 found to be mimicked and synthesized by eukaryotic cells(26). Research has
92 demonstrated that several bacterial species exhibit a chemotactic response to AI-
93 2, highlighting its crucial role in forming intricate multispecies communities(27).
94 Notably, AI-2 is thought to influence the bacterial community structure in the
95 mammalian gut following antibiotic-induced dysbiosis and to bolster
96 colonization resistance against specific enteric pathogens(28). Thus, it is apparent
97 that *Salmonella* communication is a key to its pathogenesis. Despite these
98 findings, significant gaps remain in understanding the advantages of communal
99 living and how AI-2 signaling benefits *Salmonella* in physiologically relevant
100 conditions.

101 In our present study, we elucidate that the LuxS/AI-2 signaling cascade governs
102 the processes of the initial attachment and invasion into intestinal epithelial cells
103 *in vivo* in mice and *in vitro* by regulating chemotaxis and flagellar motility.
104 Furthermore, LuxS/AI-2 signaling assists in intracellular survival by regulating
105 the *pmrABC* operon, which provides resistance against antimicrobial peptides. As

106 an alternative approach, inhibition of AI-2 signaling in combination with
107 antibiotics reduced *Salmonella* organ burden and delayed mortality in mice
108 models. We investigated the underlying mechanism of bacterial communal living
109 and communication, driving key stages of *Salmonella* pathogenesis within the
110 host.

111 **Materials and Methods**

112 **Bacterial strains and Growth conditions-**

113 The wild-type *Salmonella* enterica serovar Typhimurium strain 14028S (STM
114 WT), generously provided by Professor Michael Hensel from the Max Von
115 Pettenkofer-Institute for Hygiene and Medical Microbiology in Germany, was
116 employed in all experiments of this study. Bacterial strains were revived on LB
117 agar, with or without antibiotics, and LB broth cultures of wild-type, knockout,
118 and complemented strains were incubated at 37°C (170 rpm) using an orbital
119 shaker. Wherever necessary, antibiotics were used, including Kanamycin (50
120 µg/ml), Chloramphenicol (25 µg/ml), and Ampicillin (50 µg/ml).

121 **Bacterial gene knockout and strain generation**

122 *Salmonella enterica* serovar Typhimurium strain 14028 and isogenic mutants
123 were used for all experiments. *luxS*, *lsrB*, *lsrK,* and *lsrR* gene knockout and *luxS*
124 complement strains were made in our previous study **(S Table 1)**. Briefly, all the
125 knockout generation was done as described previously in one gene step

126 chromosomal gene inactivation method demonstrated by Datsenko and Wanner
127 (29).

128 Briefly, for the complement strain, the double-digested PCR amplified purified
129 *luxS* gene (containing BamH1 and HindIII restriction site sequences) was used to
130 clone in double-digested pQE-60. The respective ligated vector was transformed
131 into the STM Δ*luxS* strains to generate the complement strains. For the reporter
132 plasmid *plsr*-GFP generation, 256 bp of upstream of *lsrA* were cloned into the
133 promoter less vector pUA66. Finally, the reporter plasmid was transformed into
134 the STM WT and STM Δ*luxS*.

135 **Cell culture and maintenance**

136 Caco-2 epithelial cell lines were maintained in Dulbecco's Modified Eagle
137 Medium (DMEM, Lonza), supplemented with 10% FBS (Gibco), 1% non-
138 essential amino acids, 1% sodium pyruvate, and 1% penicillin-streptomycin
139 (Sigma-Aldrich) in a humidified incubator with 5% CO2 at 37 °C. The cells were
140 seeded into the respective cell culture plates for each experiment to conduct
141 intracellular survival assays and intracellular gene expression experiments.

142 **Gentamicin protection assay**

143 Caco-2 cells were seeded in tissue culture plates for infection. Cells were infected
144 with STM WT, STM Δ*luxS,* STM Δ*lsrB,* STM Δ*lsrK,* STM Δ*lsrR,* and
145 *STMΔluxS:luxS* (log phase culture growing overnight in LB broth). The
146 multiplicity of Infection (MOI) 20 was used for the intracellular survival assay

147 and *Salmonella* gene expression study (qRT-PCR). Following the infection of
148 STM strains into the cell line, the plate was spun for 5 minutes at 600 rpm using
149 a Rota-Superspin R–NV swing bucket centrifuge. After that, the plate was
150 incubated for 25 minutes at 37 °C with 5% CO_2 in a humidified incubator. Then,
151 the infected cells were washed with 1X PBS twice and treated with a 100 µg/ mL
152 concentration of gentamycin. After 1 hour, the media were changed with a
153 reduced concentration of gentamycin (25 µg/ mL) and incubated until time point.
154 The time points 2h, 6h, and 16h were taken for the qRT-PCR sample and 2h and
155 16h for the intracellular survival assay.

156 DPD supplementation (of 25 µM, 50 µM,100 µM, and 200µM DPD) or spent
157 media of STM WT collected at 3h in LB growing treated STM Δ*luxS,* and
158 LuxS/AI-2 signaling inhibition(30, 31), the inhibitor (Z)-4- bromo-5-(
159 bromomethyllene)-3-methylfran-2(5H), known as BF-8 treatment, was given to
160 the STM WT culture, which was used for the gentamycin protection assay to
161 study the adhesion, invasion, and intracellular proliferation of STM.

162 **Invasion and intracellular survival assay**

163 The cells were lysed with 0.1% triton-X 100 in PBS at specific time points post-
164 infection. For the invasion, CFU was determined at 2h post-infection samples
165 and CFU in pre-inoculum. Percent invasion was calculated by using the formula-
166 [CFU at 2 hours]/ [CFU of pre-inoculum] ×100**.** For the fold proliferation, CFU

167 was determined at 2h and 16h post-infection samples. Fold proliferation was
168 determined using the formula [CFU at 16 hours]/ [CFU at 2 hours].

169 **Adhesion assay**

170 Adhesion assay was done as gentamycin protection assay with modification.
171 Infections were given to Caco-2 cells at MOI 20 and incubated for 10 minutes at
172 37 °C in a humidified incubator with 5% CO2. Thereafter, washing with 1X PBS
173 twice to eliminate any loosely adherent bacteria. After lysing the mammalian
174 cells with 0.1% Triton-X 100, samples were taken to release the bacteria into the
175 sample. After the collected samples were plated on LB agar plates at the
176 appropriate dilutions and incubated at 37 °C, the CFUs were enumerated. The
177 following formula was used to calculate the percentage adhesion = [(CFU at 10
178 min post-infection)/(CFU of the pre-inoculum)]× 100.

179 ***In vitro* motility assay-**

180 2 µl of bacterial culture was spotted onto the agar plates supplemented with 1%
181 casein enzyme hydrolysate, 0.5% yeast extract, 0.5% NaCl, and 0.5% glucose
182 with 0.3 % agar (swim agar plates) and 0.5% agar plates (swarm agar plates). The
183 swim agar plates were incubated at 37˚C for 6h, and swarm agar plates were
184 incubated for 12h. The diameters of the motility halos were measured at least
185 three angles of three replicate plates, and then images were taken using a BioRad
186 chemidoc.

187 **Chemotaxis assay-**

188 Chemotaxis assay was done by using μ-Slide Chemotaxis, ibidi. μ-Slide consists
189 of two distinct opposing liquid chambers or reservoirs separated by a small liquid
190 transition zone of 1 mm. Overnight grown STM WT, STM Δ*luxS*, and STM Δ*lsrB*
191 were followed by two washes with motility buffer (MB; 10 mM KPO4, 0.1 mM
192 EDTA, and 67 mM NaCl, pH 7), and then resuspension to a final OD600 to 0.3
193 in MB supplemented with 3.5% glucose (MBg)(24). To reduce metabolic
194 activity, cells were chilled for 20 minutes. A motility buffer was applied to the
195 transition zone. The first reservoir was completely filled with the bacterial cell
196 suspension, the second reservoir with STM WT spent media (Collected at 3h of
197 LB growth), synthetic DPD molecule, and the known chemoattractant L-serine.
198 In a different experiment, the numbers of bacteria that transmigrated from the first
199 reservoir into the second reservoir were quantified by CFU analysis and bright
200 field microscopy (Leica microscope SP8 falcon, 63X).

201 **RNA isolation and RT-qPCR**

202 For the gene expression study in Luria Bertani (LB) media, overnight-grown
203 culture in LB media was subjected to a subculture (at 1:100) in LB. At 3h, 6h,9h,
204 and 12h, bacterial cell pellets were collected in TRIzol (from TaKaRa, RNA
205 isoPlus- 9109) and kept at -80˚C. Total RNA was isolated by chloroform
206 extraction followed by Isopropanol precipitation. To evaluate the quality, the
207 amount of RNA was quantified in nano drops and examined on a 2% agarose gel.
208 To produce cDNA, 2 μg of RNA sample was treated with DNase I at 37˚C for 1

209 hour (TaKaRa), followed by heating for 10 minutes at 65˚C. Then, DNA-free
210 RNA samples were used to make cDNA by using the PrimeScript RT reagent Kit
211 provided by TaKaRa (Cat# RR037A).
212 The gene expression of *Salmonella* upon Infection in Caco-2 infection was given
213 at MOI 20. At 2h, 6h, and 16h post-infection, samples were collected in TRIzol
214 (from TaKaRa, RNA isoPlus- 9109) and kept at -80˚C. Total RNA isolation and
215 cDNA were synthesized using a similar protocol described in the kit provided,
216 TRIzol (from TaKaRa, RNA isoPlus-9109) and TaKaRa (Cat# RR037A)
217 reagents according to the manufacturer's protocol. The list of expressions Primer
218 is provided in **S Table 2**. Quantitative PCR was carried out using a SYBR Green
219 Q-PCR kit (Takara), and the ΔΔCt method was used for quantification.

220 **RNA sequencing and analysis**

221 Bacteria were grown till mid-log phase and RNA extraction was performed using
222 Qiagen RNeasy Mini kit (Cat. No. 74104) with a few modifications. The RNA
223 samples were quantified on Nanodrop and Qubit flurometer using appropriate
224 standards. Appropriate dilutions were loaded on a High sensitivity RNA screen
225 tape and run on Agilent Tape station 4200 to determine the RNA integrity number
226 (RIN). For Library preparation, 1000ng of RNA sample was used for
227 ribodepletion by using NEB Next rRNA depletion kit Bacteria (Cat. no. NEB
228 E7850X), which includes Probe hybridization of RNA, RNase H digestion,
229 DNase 1 digestion according to the manufacturer's protocol. The NEBNext®

230 Ultra II Directional RNA Library prep kit for Illumina (Cat. no. E7760L), was
231 used to construct double-stranded cDNA libraries from the rRNA depleted RNA,
232 using RNA fragmentation, first strand cDNA synthesis with random primers,
233 second strand cDNA synthesis, end repair of double stranded cDNA, adapter
234 ligation, removal of excess adapter using sample purification beads, PCR
235 enrichment of adapter ligated DNA and clean-up of PCR products as instructed
236 by the manufacturer. The cleaned libraries were quantified on Qubit®flurometer
237 and appropriate dilutions loaded on a D1000 screen tape to determine the size
238 range of the fragments and the average library size.

239 The original raw data from the Illumina platform is transformed into sequenced
240 reads by base calling. Raw data are recorded in a FASTQ file containing sequence
241 information (reads) and corresponding sequencing quality information. The
242 quality of the reads was assessed using Fast QC v 0.11.9 before proceeding with
243 the downstream analysis(32). The reads were passed through SortMeRNAv4.3.7
244 (33) and were used against all eight rRNA databases provided to filter and remove
245 rRNA reads. The trimmed reads were then passed through fastp (34) to remove
246 adaptors, low-quality bases (Q< 36 bp). For mapping and quantification,
247 *Salmonella* Typhimurium 14028s reference genome and annotation were
248 downloaded from (https://ftp.ncbi.nlm.nih.gov/genomes/all/GCF/000/022/165/
249 GCF_000022165.1_ASM2216v1/). HISAT2 (35) was used to create the reference
250 index, and the trimmed & filtered reads were mapped to the indexed genome

251 using HISAT2. Quantification was performed with feature Count (36). A total of
252 4728 features were assigned in the raw count file. The raw count file is made into
253 raw counts for individual sets, and the rest of the differential analysis is done
254 according to the sets. The library sizes are plotted for individual sets. The
255 transcripts with low read counts (< count of at least 10 for a minimum of 2
256 samples) were removed. The filtered read counts were normalized by
257 transforming to the rlog transformation function (rlog) of DESeq2 (37) and are
258 used for further analysis. Differential gene expression was analysed using the
259 DESeq function from the DESeq2 package with a false discovery rate (FDR) cut-
260 off of ≤ 0.05 and a minimum expression log2-fold change (FC) of ≥ 2/1. The
261 counts are illustrated with a volcano plot. The top genes with the largest log2fold
262 change are plotted as a heatmap.

263 **Transmission electron microscopy**

264 Flagella were visualized using the protocol described previously(38, 39). Briefly,
265 overnight bacterial cultures were subcultured in LB media and incubated until it
266 reached an OD of 0.1. During the subculture, STM WT was treated with AI-2
267 signaling inhibitor BF-8, and STM Δ*luxS* with STM WT spent media and
268 synthetic DPD. The bacterial cultures were centrifuged at 2000 rpm for 10 min at
269 4◦C. The bacterial cells were washed with 1XPBS twice, and finally, the cells
270 were resuspended in 100 µl of 1X PBS. 10 µl of the cell suspension was added

271 on a copper grid, air dried, stained with 1% uranyl acetate for 30 s, and visualized
272 under a transmission electron microscope (Thermo-Fischer Scientific).

273 **Immunofluorescence**

274 After appropriate post-infection incubation time in the adhesion assay, the media
275 was removed, and the cells were washed with 1X PBS and fixed with 3.5%
276 Paraformaldehyde for 10 min. The cells were then washed with 1X PBS,
277 incubated with the required rabit-raised anti-*Salmonella* primary antibody in a
278 buffer containing 2% BSA, and incubated for 1 hour at room temperature or
279 overnight at 4°Cmin. After washing with 1X PBS, the secondary antibody tagged
280 to a fluorochrome was added and incubated. For Caco-2 epithelial cells, FM464
281 dye was used. The coverslips were washed with PBS, mounted on a clean glass
282 slide using mounting media containing an anti-fade reagent, and observed under
283 the confocal microscope (Leica microscope SP8 falcon, at 63X oil immersion).

284 Mice intestine histochemistry samples were incubated with the required rabbit-
285 raised anti-*Salmonella* primary antibody in a buffer containing 0.01% saponin
286 and 2% BSA, and incubated for 1 hour at room temperature or overnight at
287 4°Cmin. After washing with 1X PBS, the secondary antibody tagged to a
288 fluorochrome was added and incubated for 1h at room temperature. The dye
289 DAPI was used to stain the intestinal nucleus. 40X oil immersion was used to
290 study the mice intestine histopathology (Zeiss 710 microscope, at 63X oil
291 immersion).

292 **Polymyxin treatment and survival assay**

293 Polymixin MIC was determined by using microbroth dilution methods.
294 Polymixin treatment (sub-MIC concentration 0.5 µg/ml) was given to the
295 overnight STM strains (10^7 cfu) in LB media. At 3h post-treatment, CFU was
296 determined by spread plate methods. For the time-dependent survival assay, we
297 collected the treated sample at 3h, 6h, 9h, and 12h and calculated the CFU. For
298 the mRNA expression study, samples were collected during mid-log phase (6h)
299 in Trizol and kept at -80°C for further RNA isolation.

300 **Flow cytometry**

301 Reporter strain STM WT-*plsr*-GFP and STM *ΔluxS-plsr*-GFP were grown in LB
302 media, and samples were taken out at different time points and fixed with 3.5%
303 paraformaldehyde. The positive GFP percentage population was determined in
304 the sample by using BD FACS Verse.

305 ***In vivo* animal experiment**

306 Male C57BL/6, aged 5 to 6 weeks, were obtained from the Central Animal
307 Facility, IISc.

308 **Invasion assay**- 5–6 weeks old C57BL/6 mice were infected by orally gavaging
309 107 CFU of STM WT, STM *ΔluxS*, STM *ΔlsrB*, STM *ΔlsrK*, STM *ΔlsrR,* and
310 STM *ΔluxS:luxS*. For invasion assay intestine was isolated 6 h post-infection, and
311 CFU was enumerated on differential and selective SS agar by serial dilution

312 followed by plating. BF-8 (10 μg/ml) treated STM WT culture and DPD
313 supplementation (100 μM DPD) or STM WT spent media treated STM Δ*luxS* was
314 used for invasion study in mice.

315 ***In vivo*, competition assay-** Competition assay was done between STM WT and
316 STM*ΔluxS*/STM*ΔlsrB*/STM*ΔlsrK*. Infection was given by oral gavage with 107
317 CFU/ml of culture in a 1:1 ratio. Post five days of infection, the intestine (Peyer's
318 patches), MLN (mesenteric lymph node), spleen, liver, and blood were
319 aseptically extracted to examine the colonization in the organs. The CFU was
320 enumerated on differential and selective *Salmonella-Shigella* (SS) agar and
321 respective antibiotics containing LB agar plates. The competitive index was
322 calculated for a WT strain and knockout strains by dividing the ratio between
323 CFU (Knockout strain) and CFU (STM WT) by the ratio of both strains in the
324 inoculum.

325 ***In vivo* infection and BF-8/antibiotics treatment**- 5–6 weeks old C57BL/6 mice
326 were infected by orally gavaging 10^7 CFU of STM WT. Post 3rd day of infection,
327 one cohort of mice was sacrificed for the organ burden of *Salmonella*. The rest of
328 the cohort of mice were treated with either 2mg/kg of body weight of BF-8,
329 ciprofloxacin, ceftazidime, or a combination of BF-8 with both antibiotics
330 intraperitoneally for three consecutive days. After the 3rd day of treatment, mice
331 were sacrificed the next day, and the organ burden was determined by CFU
332 enumeration.

333 **Mice survival assay**

334 The mice were given 10^7CFU of STM WT (overnight grown cultures) orally to
335 compare the survival and weight alterations of mice post-infection and BF-8
336 /antibiotics treatment. Post 3rd day of infection, mice were treated with either
337 2mg/kg of mouse weight of BF-8, ciprofloxacin, ceftazidime, or a combination
338 of BF-8 with both antibiotics, intraperitoneally for three consecutive days. The
339 mice were observed every day to determine their survival and weight, and the
340 results were expressed as a percentage of survival (Kaplan-Meier curve) and
341 weight reduction.

342 All experiments comply with the rules set forth by the Indian Institute of Science,
343 Bangalore's IEAC. The approved protocol number is CAF/ Ethics/852/2021. The
344 Institutional Animal Ethics Committee approved every animal experiment, and
345 the National Animal Care Guidelines were scrupulously followed.

346 **Statistical analysis**

347 As mentioned in figure legends, each experiment has been independently
348 repeated two to five times. GraphPad Prism 8.4.3 was utilized for all statistical
349 analyses. As the figure legends state, the statistical analyses included an unpaired,
350 two-tailed Student's t-test, One-way ANOVA with Dunnet's post hoc test, Two-
351 way ANOVA with Tukey's post hoc test. A non-parametric one-way ANOVA
352 (Kruskal Wallis) test with Dunn's post-hoc test was performed for the animal
353 experiment. P-values less than 0.05 were regarded as significant. The analysis is

354 presented as mean ±SD or mean ±SEM with information on group sizes and p

355 values mentioned in the respective figure legends.

356

357 **Results**

358 **Autoinducer-2 signaling governs bacterial motility and flagellar**
359 **organization by modulating chemotaxis and flagella-related genes**

360 We first investigated whether *Salmonella* LuxS/AI-2 signaling is involved in
361 motility. As reported, the aggregation of *E. coli* towards AI-2 depends on motility
362 and chemotaxis(24),we have also observed that upon deletion of *luxS*, *lsrB*, and
363 *lsrK*, swim and swarm motility were hampered compared to STM WT **(Fig.1A,**
364 **B; S1A, B)**.

365 Many motile bacteria control their swimming direction by regulating the sense of
366 flagellar rotation in response to sensory cues. FliM is a key component of the
367 flagellar motor's switch complex, along with FliG and FliN, which is thought to
368 interact with one of the chemotaxis proteins, CheY(40, 41). The result of these
369 interactions is to induce clockwise rotation of the flagellar motors and tumbling
370 of the cell. We hypothesized that Lux/AI-2 signaling, due to its virtue of
371 orchestrating gene expression, might regulate the expression of these genes to
372 modulate motility. We observed that *in vitro* LB media, *fliM*, *cheY,* and *motA*
373 (regarded as the stator of the flagellar motor)(42), mRNA expression was
374 downregulated in STM *ΔluxS*, STM *ΔlsrB*, STM *ΔlsrK* compared to STM WT
375 **(Fig.1C-E)**. Following this, we noted that genes involved in transcription
376 regulation of flagella assembly *flhD, fliA, fliC, fljB*,(43) were also downregulated
377 in the absence of AI-2 accumulation and phosphorylation **(S1 C-F)**. We further
378 observed that in the absence of AI-2 sensing and signaling, the number of flagella

379 is reduced on the surface of STM *ΔluxS* and STM *ΔlsrK*, while there were no
380 flagella on the surface of *STM ΔlsrB*. We further validated with inhibition of AI-
381 2 signaling using BF-8, a competitive inhibitor of DPD in STM WT and
382 supplementing with exogenous DPD and STM WT spent media to STM *ΔluxS.*
383 We observed that BF-8 treatment reduced and DPD or spent media treatment
384 increased the flagella number (Fig.1F). From these data, we concluded that
385 LuxS/AI-2 signaling governs motility and flagellar organisation via regulating
386 flagella and chemotaxis-related gene expression.

387 **AI-2 sensing in *Salmonella* assists in chemotaxis and enhances the**
388 **attachment to Caco-2 epithelial cells**

389 Studies show that in *E.coli,* AI-2 binds LsrB, and L-serine binds Tsr
390 chemoreceptor, and both LsrB and Tsr are necessary for sensing AI-2, but not for
391 AI-2 uptake. This suggests that LsrB and Tsr interact directly in the periplasm
392 within *E.coli*(27). We speculate that the LsrB receptor in *Salmonella* may act as
393 a chemoreceptor and aid in the attraction to the AI-2 molecule. We used a μ-Slide
394 Chemotaxis chamber (ibidi) for the chemotaxis assay. DPD, STM WT spent
395 media, and serine were used in the second reservoir of the chamber. Serine was
396 used as a positive control as a chemoattractant. We found that the number of STM
397 WT transmigrated towards spent media, DPD, and serine was higher compared
398 to STM *ΔluxS* and STM *ΔlsrB* **(Fig.2 A-C)**. The explanation for the reduced
399 transmigration of STM *ΔluxS* and STM *ΔlsrB* toward serine is due to reduced

400 flagella activity. These data suggest that LuxS/AI-2 signaling controls flagellar
401 motility and chemotaxis.
402 Replicating laboratory conditions that accurately reflect the natural microbial
403 habitat during infection presents significant challenges. Consequently, fluid flow,
404 a defining characteristic of natural environments, is often ignored in experimental
405 setups. However, with the development of microfluidic technology coupled with
406 high-resolution imaging, it is now possible to understand environmental features
407 that affect bacterial pathogenesis(44). But this natural flow can remove the
408 autoinducer molecule and hamper the signaling. A study revealed that *S. aureus*
409 produces enterotoxin B in crypts, deepening them and insulating the bacteria from
410 flow, facilitating QS-regulated pathogenicity(45). Similarly, *V. cholerae* activates
411 QS within, but not outside, intestinal crevices, highlighting the role of topography
412 in virulence(46, 47). *Salmonella* is a pathogen that primarily infects the ileum,
413 the distal part of the small intestine(48). *Salmonella* has evolved mechanisms to
414 gain access, attach, and infect the intestinal epithelial cells of the crypt to survive
415 and replicate. We speculate that *Salmonella* is attracted towards AI-2 molecules
416 of the intestinal crypts, where fluid flow is resisted, and it can answer why
417 *Salmonella* moves to the distal part of the intestine. Epithelial cells release an AI-
418 2 mimic in response to bacteria, and bacteria might benefit from this AI-2 mimic
419 via their AI-2 quorum-sensing receptors(26). We were curious whether LuxS/AI-
420 2 modulates the attachment to epithelial cells. Our adhesion assay suggests that
421 STM *ΔluxS*, STM *ΔlsrB*, and *ΔlsrK* compromised their ability to adhere to Caco-

422 2 epithelial cells **(Fig. 2D, E, S2A).** On the other hand, STM *ΔlsrR* behaves
423 similarly to STM WT. Upon inhibition of LuxS/AI-2 signaling with BF-8 in STM
424 WT and exogenous DPD and STM WT spent media treatment to STM *ΔluxS,* AI-
425 2 sensing and signaling enhance the attachment to epithelial cells **(Fig. 2F).**

426 ***Salmonella* exploits its LuxS/AI-2 mediated communication to invade**
427 **intestinal epithelial cells**

428 Adhesion and invasion represent the crucial step of successfully establishing
429 infection by bacterial pathogens and cellular invasion, which is followed by
430 intracellular multiplication, dissemination to other tissues, or persistence(39, 49,
431 50). Having observed that LuxS/AI-2 enhances the attachment to Caco-2 cells,
432 we also conjecture that LuxS/AI-2 signaling regulates the invasion of *Salmonella*
433 into the epithelial cells. We infected the Caco-2 epithelial cell with STM stains
434 and observed that STM WT, *luxS* complemented in STM *ΔluxS,* and STM *ΔlsrR*
435 invade more efficiently compared to STM *ΔluxS*, STM *ΔlsrB*, and *ΔlsrK* **(Fig.**
436 **3A)**. Further, we treated the STM *ΔluxS* with exogenous DPD and STM WT spent
437 media and STM WT with inhibitor BF-8 followed by infection in Caco-2
438 epithelial cells. Exogenous DPD and spent media treatment recovered the
439 invasion compared to untreated STM *ΔluxS,* while upon inhibition with BF-8, the
440 STM WT invasion was reduced **(S3 A-C)**. Next, to validate our *in vitro* cell line
441 results, we then studied the invasion of the knockout strains into the intestine of
442 C57BL/6 mice **(Fig. 3B).** Interestingly, STM *ΔluxS*, STM *ΔlsrB*, and *ΔlsrK*
443 invaded significantly less into the Peyer's patches of the C57BL/6 mice **(Fig. 3C)**.

444 STM WT invasion was reduced upon BF-8 treatment. In contrast, STM *ΔluxS*
445 invasion increased with the treatment of DPD and STM WT spent media **(S4A)**.
446 The immunofluorescence study with the histopathological sections of the mouse
447 ileum further validated the reduced invasion and colonization of the mutants in
448 the intestine **(Fig. 3D; S4B)**.
449 It is shown that the master regulator HilD regulates *Salmonella* invasion and
450 motility via activating gene expression of the type 3 secretion system 1 (SPI-1)
451 and motility genes(51, 52). We hypothesized that LuxS/AI-2 signaling regulates
452 the *hilD* and other SPI-1 master regulators to modulate the invasion or infection
453 in host cells. We observed that *hilD, hilA,* and *invF* master regulators of SPI-1
454 were downregulated in STM *ΔluxS*, STM *ΔlsrB*, and STM *ΔlsrK in vitro* LB
455 media compared to STM WT **(Fig. 4 E-G)**. Thus, *Salmonella* requires LuxS/AI-
456 2 signaling to invade successfully within the IECs *in vitro* and *in vivo* via
457 regulating SPI-1 regulators.
458 **LuxS/AI-2 signaling is active and facilitates survival within Caco-2 epithelial**
459 **cells**
460 As the LuxS/AI-2 signaling is a key language for *Salmonella* communication, ,
461 we sought to explore its role in the next stages of infection. To begin, we asked
462 how *Salmonella* Typhimurium regulates the expression of the genes within the
463 *lsr* operon and *luxS* upon infection into host cells? We evaluated the mRNA
464 expression of *luxS* and *lsr* operon genes (*lsrB*, *lsrK*, *lsrR*) in STM WT upon
465 infection in the Caco2 cell line. We noted that the *lsr* operon genes were slightly

466 higher at post 6h infection compared to 2h post-infection, and further, it
467 downregulated at late 16h post-infection **(Fig. 4A)** while *luxS* expression was
468 similar at 2h and 6h post-infection and downregulated at 16h post-infection
469 compared to 2h **(Fig. 4B)**. Consistent expression of genes suggests that AI-2
470 signaling may be active inside the host cell. Following this, we observed that
471 STM *ΔluxS*, STM *ΔlsrB*, and STM *ΔlsrK* proliferate less in comparison to STM
472 WT, STM *ΔlsrR,* and *luxS* complemented STM *ΔluxS* within the Caco-2 cells
473 **(Fig. 4C)**. The fold replication was reduced in the BF-8-treated culture of STM
474 WT **(Fig. 4D)**. Conversely, upon treatment of WT spent media and exogenous
475 DPD molecule, STM *ΔluxS* fold replication was recovered **(S5A, B)**. To further
476 confirm whether this signaling is active inside the host cells, we generated the
477 reporter strain, which produces green fluorescence on LuxS/AI-2 activation.
478 Firstly, we checked the quorum sensing active bacteria during the *in vitro* growth
479 in LB media. Flow cytometry and fluorescence microscopy results suggest that
480 quorum-sensing active bacterial cells were increased in mid-log phase to early
481 stationary phase **(Fig. 4E; S5C)**. Moreover, when we gave the STM WT spent
482 media treatment to STM *ΔluxS* (Containing reporter construct), we observed that
483 STM *ΔluxS* became quorum sensing active (**S5D)**. Upon infection in Caco-2
484 epithelial cells with reporter STM strain suggests that Lux/AI-2 signaling is active
485 inside the host cells **(Fig. 4F)**. Taken together, this suggests that LuxS/AI-2
486 signaling is active and facilitates survival within Caco-2 epithelial cells.

487 **LuxS/AI-2 cascade facilitates *Salmonella* survival by evading host**
488 **antimicrobial peptide defence mechanisms**

489 The innate immune system within the gut relies substantially on antimicrobial
490 peptides (AMPs) from epithelial cells, including cathelicidins and defensins.
491 They help maintain intestinal homeostasis by targeting pathogens and regulating
492 the gut microbiota(53). Our previous study showed that the LsrR repressor
493 protein negatively modulates the expression of the *phoP* gene, which protects
494 against acidic stress(54). Several studies revealed cationic antimicrobial peptides
495 can activate the PhoP/PhoQ two-component system (TCS), and the PhoP/PhoQ
496 two-component system TCS regulates the expression and activation of *pmrABD*
497 and provides protection against the AMPs (55-62). We considered that LuxS/AI-
498 2 signaling might aid in combating antimicrobial peptide sensitivity via
499 regulating *phoP/phoQ*. In continuation, we observed that STM *ΔluxS*, STM
500 *ΔlsrB*, and STM *ΔlsrK* were more sensitive compared to STM WT and STM
501 *ΔlsrR* under *in vitro* conditions in the presence of sub-MIC concentration of
502 polymyxin **(Fig. 5A; S 6A, B)**. Subsequently, we found that the mRNA
503 expression levels of *pmrD*, *pmrA*, and *pmrB* were reduced in STM *ΔluxS*, STM
504 *ΔlsrB*, and STM *ΔlsrK* compared to STM WT under polymyxin-treated
505 conditions *in vitro* in LB media **(Fig. 5B)**. However, in STM *ΔlsrR*, their
506 expression levels were comparable to those in STM WT. Thereafter, *pmrD*, *pmrA*,
507 and *pmrB* gene expression level reduction was observed upon infection in Caco-
508 2 epithelial cells in STM *ΔluxS*, STM *ΔlsrB*, and STM *ΔlsrK* compared to STM

509 WT **(Fig. 5 C-E)**. Conclusively, LuxS/AI-2 signaling facilitates survival within
510 Caco-2 epithelial cells by regulating the *pmrD/AB* gene expression.

511 **LuxS/AI-2 signaling regulates critical gene targets to assist in multiple stages**
512 **of *Salmonella* infection in the host**

513 As we observed, LuxS/AI-2 signaling is involved in various stages of *Salmonella*
514 infection by regulating multiple genes. Following this, we performed
515 transcriptomic analysis between STM WT and quorum sensing knockout strains
516 STM *ΔluxS*, STM *ΔlsrB, and* STM *ΔlsrK.* We figured out that over the 4728 gene
517 variables, 507, 1291, and 225 genes were significantly differentially expressed in
518 STM *ΔluxS*, STM *ΔlsrB,* and STM *ΔlsrK,* respectively. Out of which, 316 are
519 down-regulated and 191 are up-regulated in STM *ΔluxS,* 902 are down-regulated
520 and 389 genes are up-regulated in STM *ΔlsrB,* while 106 are down-regulated and
521 119 are up-regulated in STM *ΔlsrK* in comparison to STM WT **(Fig. 6A-C)**. Gene
522 enrichment and KEGG analysis revealed that down-regulated genes belong to the
523 flagellar classes (*fliC*/*fljB* family gene), chemotaxis (*cheY*, *motA*, *motB* etc.),
524 secretory protein and virulence-associated genes (*sopD2*, *sseI*, *pipB*, *sopB*, *sifA*)
525 etc **(Fig. 6D, E)**. Interestingly, the heatmap of the top 50 genes also includes genes
526 related to flagellar motility *fliC*/*fljB*, chemotaxis gene *motA,* and virulence genes
527 (*hilD*, *pipB*, *sseI,* etc.) **(S7A-C)**. Taken together, the transcriptomic analysis
528 suggests that the Lux/AI-2 signaling regulates multiple critical gene targets to
529 assist in multiple stages of *Salmonella* infection in the host.

530 **Inhibition of LuxS/AI-2 signaling with antibiotics reduces *Salmonella***
531 **colonization *in vivo* and enhances mice survival**
532 *Salmonella* can mediate its uptake into enterocytes by delivering effector
533 molecules through Type 3 secretion systems (T3SS). It can also be phagocytosed
534 by immune cells such as macrophages, dendritic cells, and neutrophils residing
535 in Peyer's patches. However, *Salmonella* preferentially enters specialized cells
536 called microfold cells or M-cells of the Peyer's patches in the intestinal
537 epithelium. After breaching the epithelial cells at the Peyer's patches in the distal
538 ileum, it disseminates to the liver, spleen, and mesenteric lymph node (MLN), the
539 secondary infection sites(63, 64). *Salmonella* is known to be a successful
540 pathogen that can overcome various host immune responses such as oxidative
541 stress, nitrosative stress, acidic pH, etc(65). In our recent study, STM *ΔluxS*, STM
542 *ΔlsrB*, and STM *ΔlsrK* showed less colonization and delayed mouse mortality
543 compared to STM WT infection, and upon treatment of BF-8 (4mg/kg mice body
544 weight) to STM WT-infected mice, organ burden was reduced, and mouse
545 survivability increased(54). Following this, we observed in competition between
546 STM WT with STM *ΔluxS* or STM *ΔlsrB*, or STM *ΔlsrK* in mice co-infection
547 studies, STM WT outcompeted all three mutants in the liver, spleen, MLN, and
548 intestine **(Fig. 7A, B)**. Further, we questioned whether, upon treatment with BF-
549 8 in combination with low-concentration doses (2mg/kg of each) of antibiotics
550 ciprofloxacin and ceftazidime, the infection and mortality of mice could be cured.
551 So, we first infected the mice with STM WT by oral gavage and started the

552 treatment on the 3rd day post-infection (Fig. 7C). On the 3rd day post-infection,
553 we observed organ colonization and slight weight reduction, confirming infection
554 **(S8 A-C)**. After each day of treatment of BF-8 with or without antibiotics for
555 consecutive days, on the 6th day post-infection, we noted that organ colonization
556 was significantly less with the combination of low concentration 2mg/kg of body
557 weight (of BF-8 and ciprofloxacin or ceftazidime **(Fig. 7C-F; S8D, E)**. With the
558 treatment of three doses of a combination of BF-8 with ciprofloxacin or
559 ceftazidime, started on the 3rd day post-infection, mice survived till 14 or 15 days,
560 respectively. On the other hand, low doses of BF-8 and antibiotics also delayed
561 the mortality of mice compared to the untreated mice **(Fig. 7G, H; S8 F)**.
562 Furthermore, tissue histopathology of liver and spleen, suggested that a
563 combination treatment of BF-8 inhibitor with antibiotics improved the health of
564 the mice more effectively with a less disease score (**Fig. 7I; S9)**. These data
565 suggest that the AI-2 mediated signaling is required for *in vivo* colonization of
566 *Salmonella* in mice, and signaling inhibition can be a promising strategy in
567 combination with low doses of antibiotics for treatment of *Salmonella* infection
568 in the era of emerging antibiotic-resistant *Salmonella* strains.
569

570 **Discussion**

571 Adapting its tactics and employing multiple defense systems, *Salmonella* has
572 become a potent enteric pathogen, occupying several host niches during its
573 pathogenesis. The opening moves during its pathogenesis involve the expansion
574 and competition in the gut, followed by attachment and invasion. To do so,
575 *Salmonella* must first reach the site of infection. Of the several factors,
576 chemotaxis and motility contribute majorly to such a process. Recently, it was
577 shown that AI-2, a quorum-sensing molecule, can work as a chemoattractant and
578 help in aggregation(24). Here, we showed that *Salmonella* LuxS/AI-2 signaling
579 controls motility via regulating motility, flagellar gene expression, and flagellar
580 organisation. *Salmonella* produces and releases the AI-2 molecules, which, upon
581 reaching an optimal concentration in the environment, begin to accumulate
582 intracellularly via the ABC transporter. The phosphorylation of the intracellular
583 AI-2 by LsrK is crucial for its function and orchestration of its gene targets (66).
584 Since the accumulation of AI-2 upregulates the *lsr* operon, we also observe that
585 the genes *lsrB*, *lsrK*, and *lsrR* were upregulated during the mid-log and late-log
586 phases(54). This provides an additional context to our current observations, as
587 flagella formation is primarily during its exponential growth phases *in vitro*.

588 The gastrointestinal tract is a dynamic environment where microbes compete for
589 space and nutrients through various mechanisms. Many gut-associated bacteria
590 produce AI-2 via the LuxS enzyme, including a significant proportion of
591 Firmicutes and Proteobacteria, and a few members of the phyla Bacteroidetes and

592 Actinobacteria. (67, 68). Besides, species of the families Barnesiellaceae and
593 Muribaculaceae also contribute to AI-2 production in the gut (69). Being an
594 enteric pathogen and a sensor of the universal communication signal, *Salmonella*
595 may profit from the AI-2 produced by the gut commensal in the intestinal lumen.
596 Through its ABC transporter, *Salmonella* may readily take up the extracellular
597 AI-2 produced by the gut microbes. This further demonstrates that intra-bacterial
598 communication and interactions might be exploited by pathogens to win the arms
599 race.
600 Natural fluid flow in the intestine can remove autoinducers, disrupting quorum
601 sensing. *Staphylococcus aureus* utilizes autoinducers in the crypts (non-existent
602 flow) and enhances pathogenicity by producing enterotoxin B (45). Similarly,
603 *Salmonella* targets the ileum crypts to invade epithelial cells, ensuring survival
604 and replication. Natural dynamics are crucial in bacterial adaptation and
605 virulence(48). Motility towards the ileum of the intestine is essential, and sensing
606 AI-2 plays a pivotal role in *Salmonella* pathogenesis. Our results suggest that
607 *Salmonella* can move toward the AI-2 molecule, and LsrB might work as a
608 chemoreceptor. As previously studied, LsrB in *E.coli* acts as a receptor for AI-2
609 and aids in the sensing and drives chemotaxis towards the AI-2 pool (70).
610 Similarly, we speculate that in *Salmonella,* the LsrB receptor also assists in
611 sensing AI-2, while the AI-2 is internalised through the ABC receptor, which
612 tunes the expression of chemotaxis and motility gene expression to drive motion
613 towards the AI-2 pool. HilD is the master regulator of motility and the SPI-1

614 gene. The present study shows that LuxS/AI-2 signaling regulates the *hilD* gene
615 expression, thereby aiding in motility, attachment, and invasion of epithelial cells
616 *in vitro* and *in vivo* conditions. Additionally, we observe that the SPI-1 genes *hilA*
617 and *invF* are also underexpressed in the quorum-sensing mutants. This likely
618 accounts for the impaired adhesion and invasion of these mutants, as the SPI-1
619 encoded T3SS system and effector molecule mediate host cell invasion.
620 Our findings further indicated that accumulation and phosphorylation of AI-2 are
621 necessary for controlling the expression of the *pmrD/AB*. The *pmrD/AB* could be
622 regulated by PhoP, resulting in reduced survival of STM *ΔluxS*, STM *ΔlsrB*, and
623 STM *ΔlsrK in vitro* and in the epithelial cells (71, 72). Our previous study
624 highlighted the regulatory mechanism of LuxS/AI-2 in controlling the *phoP/Q*
625 transcription (54). Hence, in such a context, our present study further highlights
626 the broader, interconnected regulatory roles of LuxS/AI-2 in several defence
627 strategies of this pathogen. Transcriptomic analysis revealed that LuxS/AI-2, the
628 language of *Salmonella,* can control various critical genes in *Salmonella.* These
629 genes are involved in flagellar motility, invasion, cell surface and membrane
630 functions, and secretory pathways. This underscores how the quorum-sensing
631 cascade regulates numerous genetic programs that are involved in the various
632 stages of *Salmonella* infection. As previously reported, the regulation of the
633 *phoP/Q* operon by the LsrR repressor through the promoter binding activity of
634 the repressor, it can be assumed that some of these genetic controls may also
635 involve the LsrR binding activity (54). Our present work also demonstrated that

636 the organ burden of *Salmonella* was reduced upon treatment of mice with
637 inhibitor BF-8 in combination with low doses of antibiotics ciprofloxacin and
638 ceftazidime. Considering the increasing emergence of antimicrobial-resistant
639 *Salmonella* strains worldwide, there is a need for alternative approaches to curb
640 infection. As we point out to the broader and interconnected regulatory
641 mechanisms by the LuxS/AI-2 signaling in *Salmonella*, intervening in such a
642 critical signaling process proves to be a promising infection resolution strategy.
643 Considering the pervasive presence of AI-2, it appears paradoxical that
644 *Salmonella* cells depend on it to colonize a specific niche within the gut. One
645 plausible rationale for this might be that AI-2 chemotaxis becomes significant
646 under dysbiosis conditions that suppress microbiota and promote the proliferation
647 of *Enterobacteriaceae* (73, 74). Our study provides evidence for a causal link
648 between AI-2 chemotaxis, gut colonization, and niche segregation of *Salmonella*
649 strains in the murine gut. It further establishes a link between AI-2 chemotaxis,
650 invasion, and colonization *in vivo*. We suggest that similar mechanisms of AI-2-
651 mediated host colonization might exist in other chemotactic enteric bacteria, and
652 inhibition of LuxS/AI-2 signaling might open avenues for antibiotic resistance of
653 pathogenic bacteria.

Data availability

The RNA-seq data generated in this study have been deposited in NCBI's Gene Expression Omnibus (GEO) and can be accessed with the GEO series accession numbers GSE305594. All the data supporting the conclusions of this study are available in the paper and supplemental materials.

Funding

This work was funded by the Department of Biotechnology (DBT), Ministry of Science and Technology, the Department of Science and Technology (DST), Ministry of Science and Technology. DC acknowledges DAE-SRC (DAE00195) outstanding investigator award and funds and ASTRA Chair Professorship funds. The authors jointly acknowledge the DBT-IISc partnership program. Infrastructure support from ICMR (Center for Advanced Study in Molecular Medicine), DST (FIST), UGC-CAS (special assistance), and TATA fellowship is acknowledged. AS duly acknowledges UGC-SRF for the financial assistance. AVN duly acknowledges the IISc-MHRD for the financial assistance.

Ethics statement

All experiments comply with the rules set forth by the Indian Institute of Science, Bangalore's IEAC. The approved protocol number is CAF/ Ethics/852/2021. The Committee for Control and Supervision of Experiments on Animals (CPCSEA), a statutory committee established under Chapter 4, Section 15 (1) of the

Prevention of Cruelty to Animals Act 1960, and National Animal Care provided guidelines that were meticulously adhered to during all animal experiments, all of which were approved by the Institutional Animal Ethics Committee. (Registration No. 435 48/1999/ CPCSEA). The Institutional Animal Ethics Committee approved every animal experiment, and the National Animal Care Guidelines were meticulously followed.

Author contribution

AS and DC conceived the study. AS and DC designed experiments. AS performed experiments. AS and AVN performed an electron microscopy experiment. RSR analyzed the tissue histopathology. AS analyzed the data, prepared the figures, and drafted the manuscript. AS, AVN, and DC reviewed and edited the manuscript. DC supervised the work. All the authors read and approved the manuscript.

Declaration of competing interest

The authors declare no conflict of interest.

Acknowledgment

The Departmental and Divisional Confocal Facility, Departmental Real-Time PCR Facility, Divisional Electron Microscopy facility, and Central Animal Facility at IISc are duly acknowledged. Mr. Arjun and Ms. Syama are acknowledged for their help with image acquisition. Ms. Kirtan is acknowledged

694 for her help with Electron microscope image acquisition. Ms. Aneesha and Ms.
695 Nanditha are acknowledged for their technical help.

696

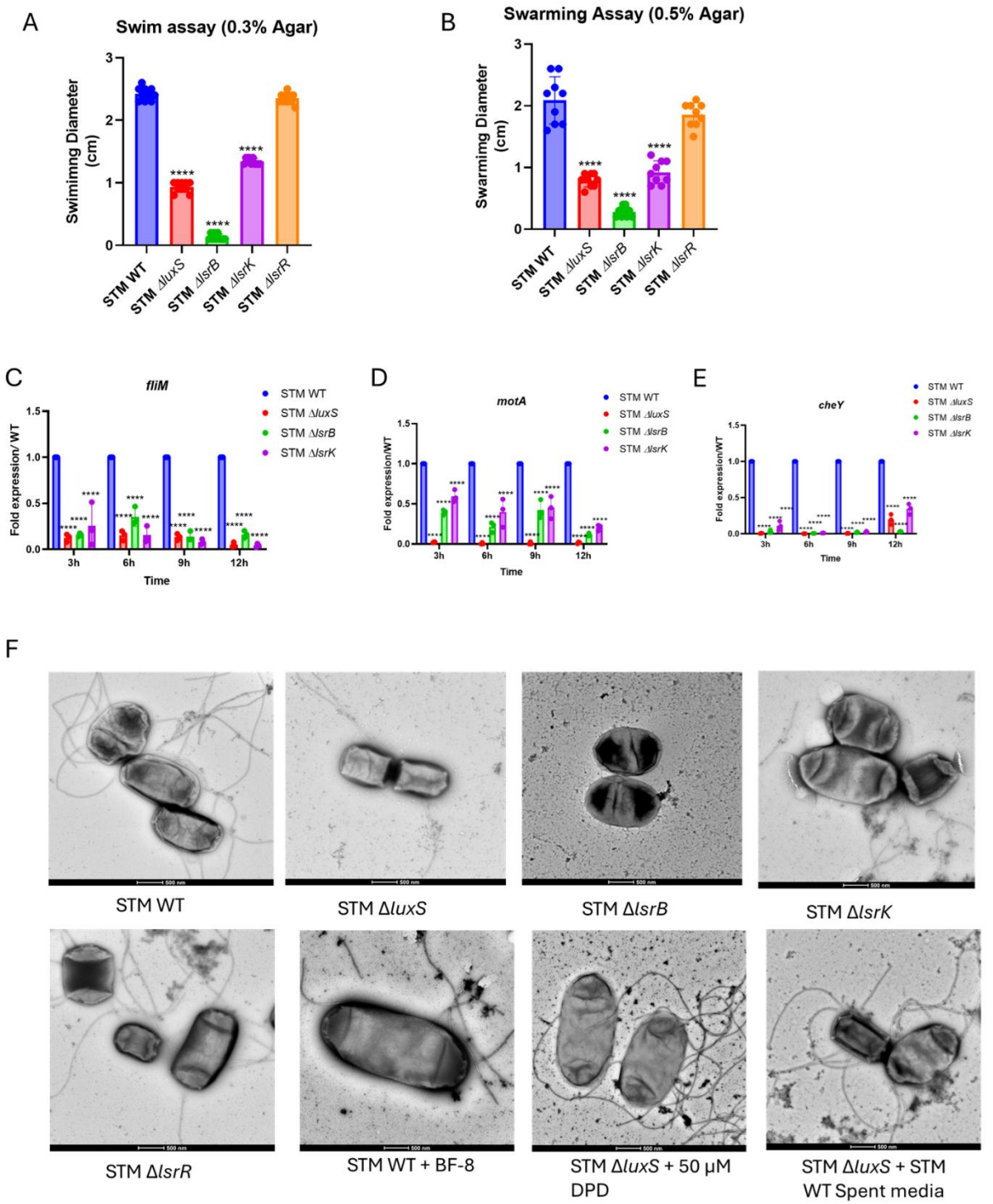

Fig.1 Autoinducer-2 signaling governs bacterial motility and flagellar organization by modulating chemotaxis and flagella-related genes. (A) Swim motility, **(B)** Swarm motility assay. Measurement has been taken at three angles per plate. Represented as Mean+/-SD of N=3, n=3. **(C)** mRNA expression of

702 *fliM*, *motA,* and *cheY* STM strains *in vitro* growth in LB. Represented as Mean+/-
703 SD of N=3, n=3, **(D)** Transmission electron microscope representative image of
704 STM strains. Represented as Mean+/-SD of N=2, n>10. One-way ANOVA with
705 Dunnet's post-hoc test was used to analyze the data; p values **** $p < 0.0001$,
706 *** $p < 0.001$, ** $p<0.01$, * $p<0.05$. Two-way Anova was used to analyze the
707 grouped data; p values **** $p < 0.0001$, *** $p < 0.001$, ** $p<0.01$, * $p<0.05$

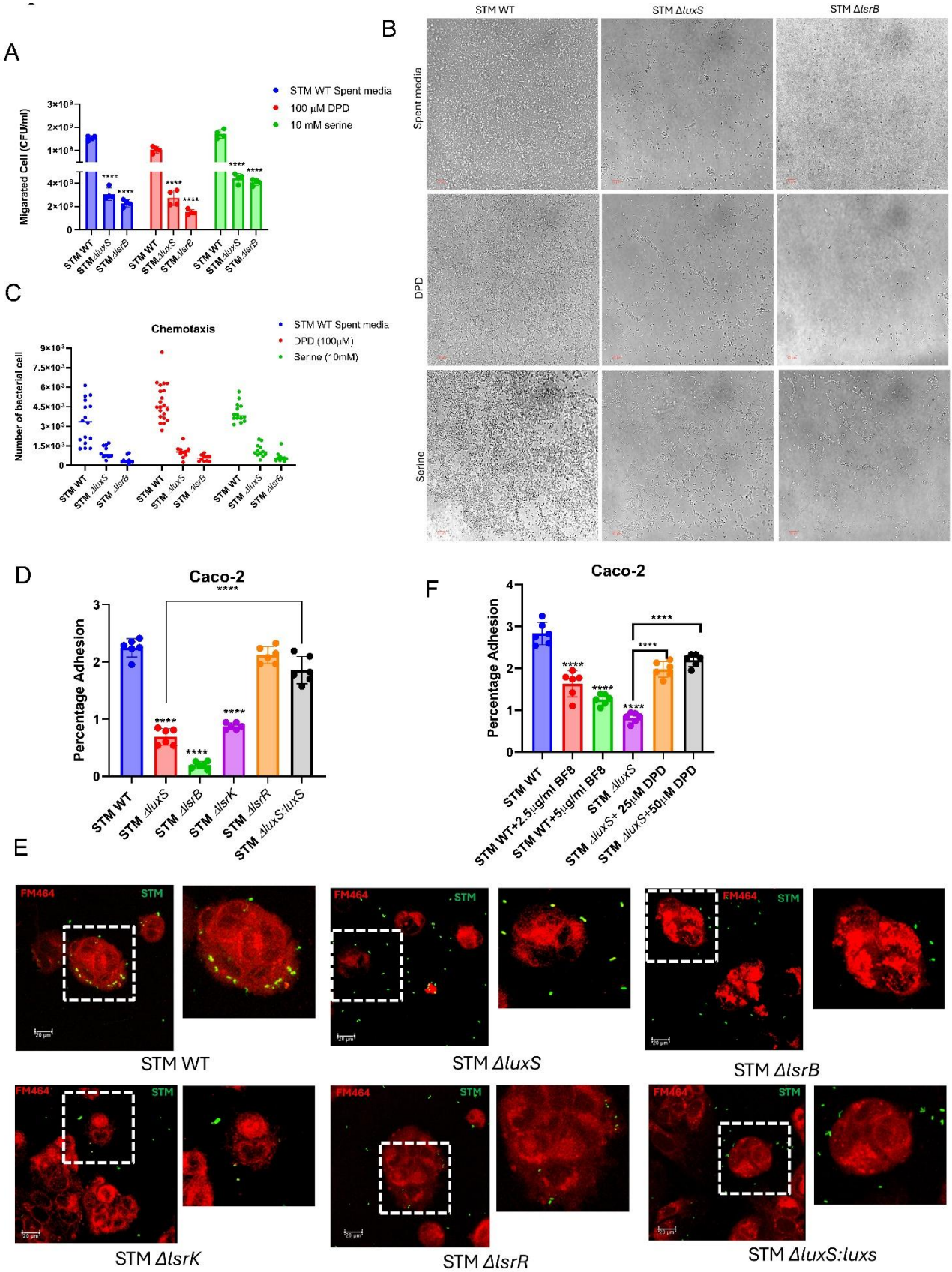
A
STM WT Spent media
100 µM DPD
10 mM serine
Migarated Cell (CFU/ml)
STM WT
STM ΔluxS
STM ΔlsrB
B
STM WT
STM ΔluxS
STM ΔlsrB
Spent media
DPD
Serine
C
Chemotaxis
STM WT Spent media
DPD (100µM)
Serine (10mM)
Number of bacterial cell
D
Caco-2
Percentage Adhesion
STM WT
STM ΔluxS
STM ΔlsrB
STM ΔlsrK
STM ΔlsrR
STM ΔluxS:luxS
F
Caco-2
Percentage Adhesion
STM WT
STM WT+2.5µg/ml BF8
STM WT+5µg/ml BF8
STM ΔluxS
STM ΔluxS+ 25µM DPD
STM ΔluxS+50µM DPD
E
FM464
STM
STM WT
STM ΔluxS
STM ΔlsrB
STM ΔlsrK
STM ΔlsrR
STM ΔluxS:luxs

708

709 **Fig. 2 AI-2 sensing in *Salmonella* assists in chemotaxis and enhances the**
710 **attachment to Caco-2 epithelial cells. (A)** CFU analysis of transmigrated STM
711 strains towards STM WT spent media, DPD, and known chemoattractant serine.
712 The experiment was performed in an ibidi chemotaxis chamber. Represented as
713 Mean+/-SD of N=3, n=2. **(B)** Bright-field microscopy images of transmigrated
714 bacteria. **(C)** Analysis of images using ImageJ software to count the number of
715 bacteria per image. Each dot represents per image. The image is represented as
716 Mean+/-SD of N=3, n>10. **(D)** Adhesion assay of STM WT, STM *ΔluxS*, STM
717 *ΔlsrB*, STM *ΔlsrK,* STM *ΔlsrR,* and STM *ΔluxS:luxS* in Caco-2 epithelial cells.
718 Represented as Mean+/-SD of N=3, n=3. **(E)** Immunofluorescence imaging to
719 study the adhesion to Caco-2 cells of STM WT and knockout strains, here
720 FM464(red) is used to stain the lipids for Caco-2, and Anti-*Salmonella* (LPS)
721 (Alexafluor-488 tagged secondary antibody used-Green) for STM.
722 Representative image of N=3, n>10. **(F)** Adhesion assay of STM WT and STM
723 *ΔluxS* treated with BF-8 and DPD, respectively. Represented as Mean+/-SD of
724 N=3, n=3. One-way ANOVA with Dunnett's post-hoc test was used to analyze
725 the data; p values **** $p < 0.0001$, *** $p < 0.001$, ** $p<0.01$, * $p<0.05$. Two-
726 way Anova was used to analyze the grouped data; p values **** $p < 0.0001$, ***
727 $p < 0.001$, ** $p<0.01$, * $p<0.05$.

728

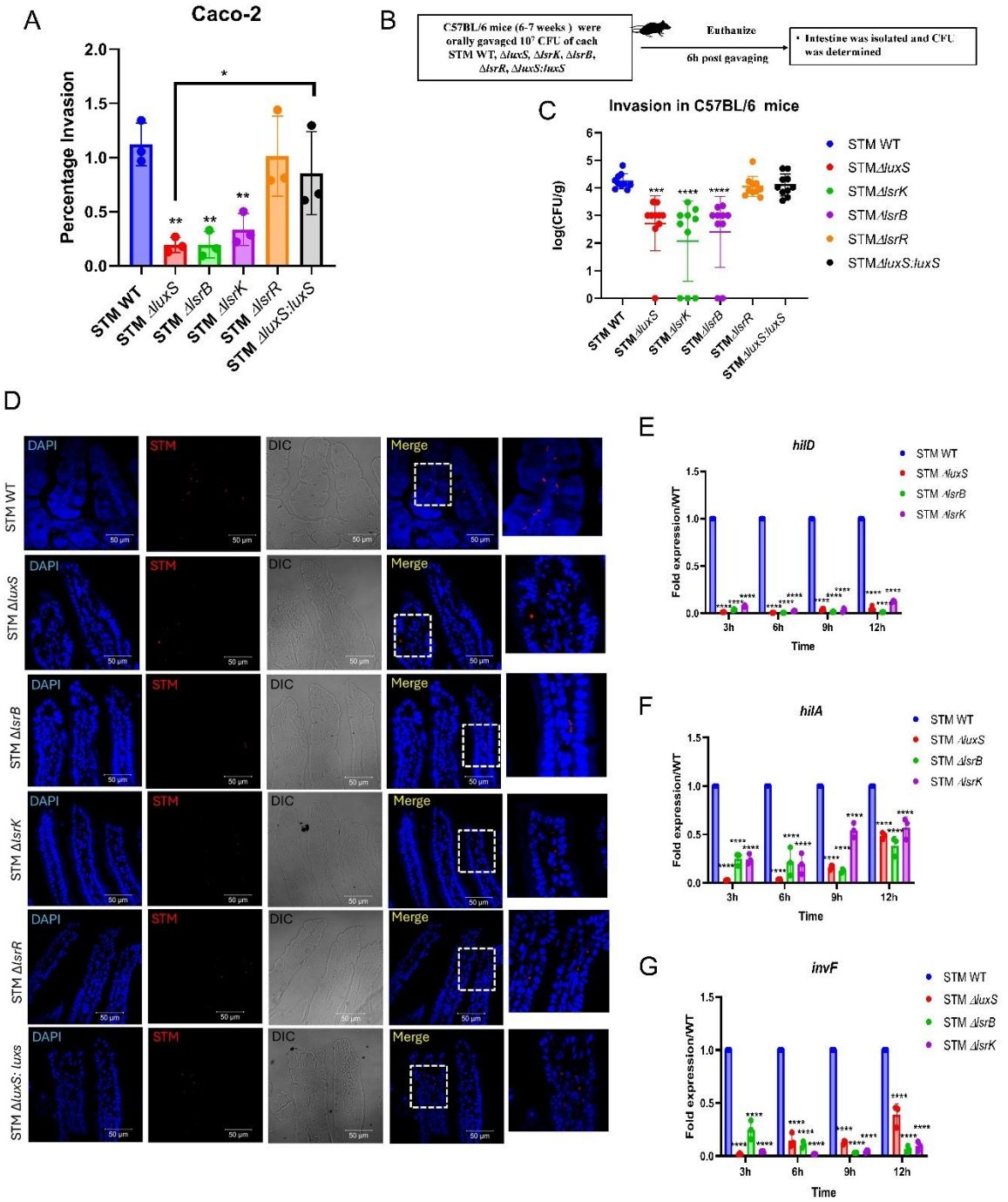

Fig. 3 *Salmonella* exploits its LuxS/AI-2 mediated communication to invade intestinal epithelial cells. (A) Percentage invasion of STM WT, STM *ΔluxS*, STM *ΔlsrB*, STM *ΔlsrK,* STM *ΔlsrR,* and STM *ΔluxS:luxS* in Caco-2 epithelial cells. Represented as Mean+/-SEM of N=3, n=3. **(B)**Experimental schematic representation of the invasion assay in C57BL/6 male mice. **(C)** STM WT, STM

735 *ΔluxS,* STM *ΔlsrB*, STM *ΔlsrK,* STM *ΔlsrR,* and STM *ΔluxS:luxS* invasion assay
736 in mice; organ burden in the intestine post 6h of infection. N=2, n=5.**(D)**
737 Immunofluorescence of histopathological sections of mice intestine (Peyer's
738 patches) to study invasion, DAPI is used to stain the nucleic acids in the cells,
739 and Anti-*Salmonella* (LPS) (Cy3 tagged secondary antibody used-Red). mRNA
740 expression of **(E)** *hilD,* **(F)** *hilA*, **(G)** *invF,* in STM WT, STM *ΔluxS,* STM *ΔlsrB*,
741 and STM *ΔlsrK in vitro* LB media. Represented as Mean+/-SD of N=3, n=3.
742 Represented as Mean+/-SD of N=2, n>10. One-way ANOVA with Dunnet's post-
743 hoc test was used to analyze the data; p values **** $p < 0.0001$, *** $p < 0.001$,
744 ** $p<0.01$, * $p<0.05$. Non-parametric One-way ANOVA (Kruskal Wallis) with
745 Dunn's posthoc test was used to analyze organ burden in mice.Two-way Anova
746 was used to analyze the grouped data; p values **** $p < 0.0001$, *** $p < 0.001$,
747 ** $p<0.01$, * $p<0.05$

748

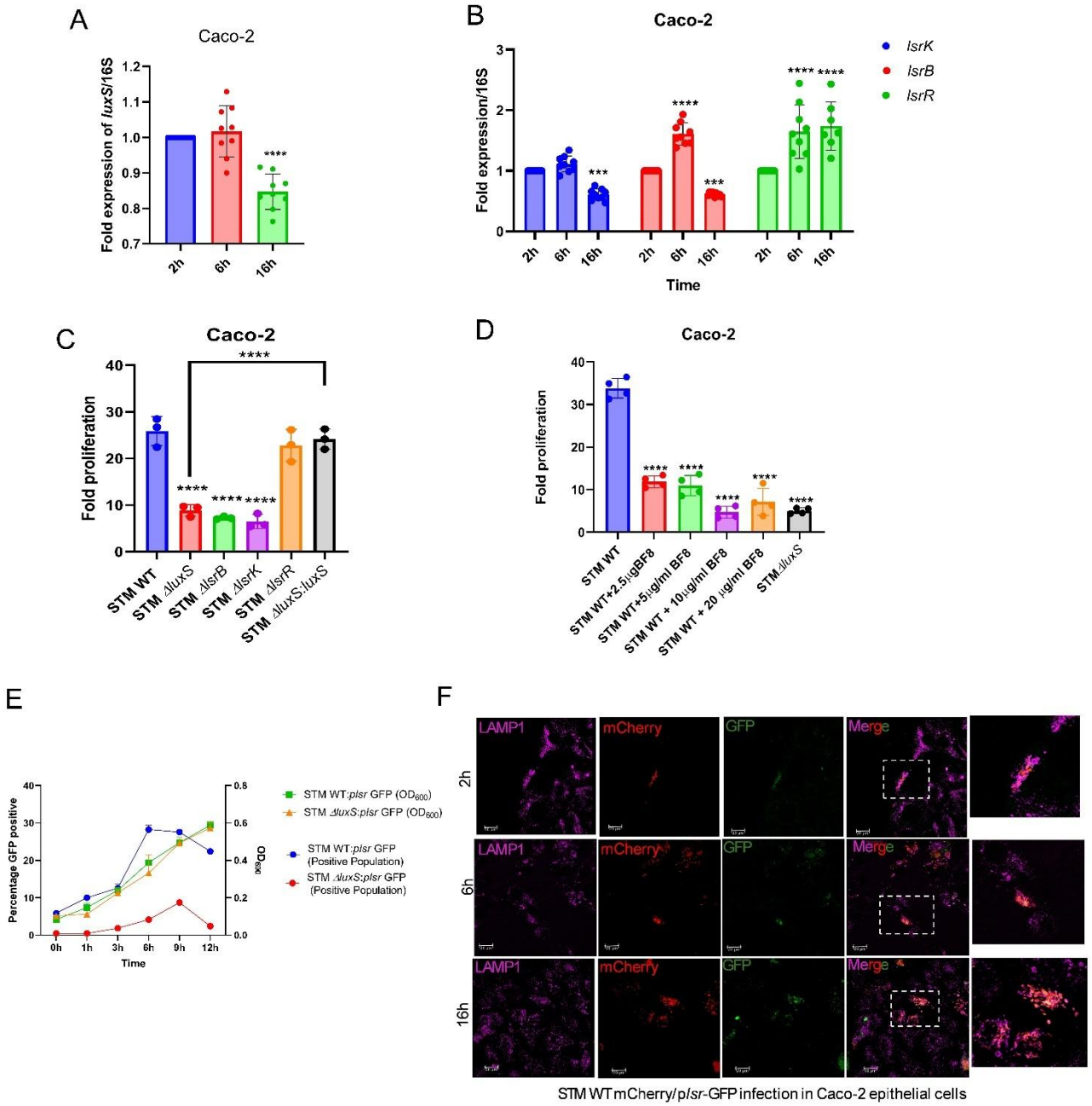

749

750 **Fig. 4 LuxS/AI-2 signaling is active and facilitates survival within Caco-2**

751 **epithelial cells**. mRNA expression of **(A)** *luxS,* and **(B)** *lsr* operon genes *lsrB*,

752 *lsrK,* and *lsrR* in STM WT upon infection in Caco-2 epithelial cells. Represented

753 as Mean+/-SDof N=3, n=3. Fold proliferation of **(C)** STM WT and knockout

754 strains, **(D)** STM WT treated with BF-8. Represented as Mean+/-SEM of N=3,

755 n=3. **(E)** Quorum sensing reporter strains growth kinetics and flow cytometry
756 analysis of GFP-positive bacterial cells. **(F)** Immunofluorescence microscopy
757 analysis of STM WT quorum sensing reporter strains upon infection in Caco-2
758 epithelial cells. LAMP1 marker- *Salmonella* containing vacuole (SCV),
759 mCherry- Constitutive expression, GFP- quorum sensing active STM. One-way
760 ANOVA with Dunnet's post-hoc test was used to analyze the data; p values ****
761 $p < 0.0001$, *** $p < 0.001$, ** $p<0.01$, * $p<0.05$. Two-way Anova was used to
762 analyze the grouped data; p values **** $p < 0.0001$, *** $p < 0.001$, ** $p<0.01$, *
763 $p<0.05$.
764

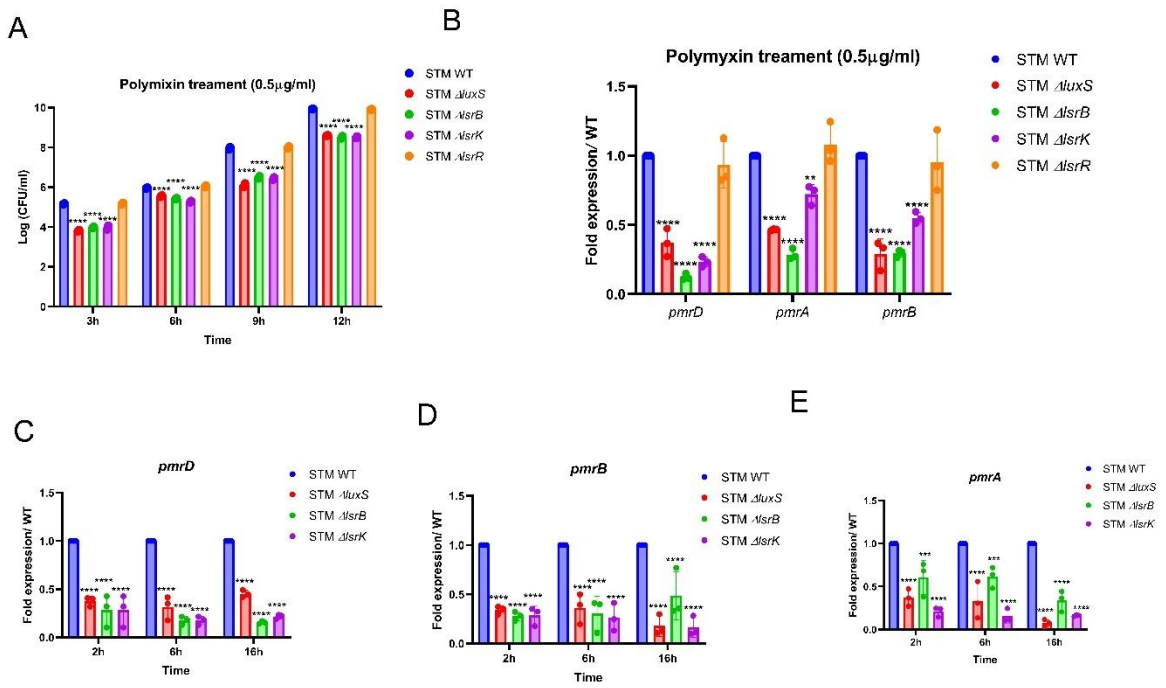

Fig. 5 LuxS/AI-2 cascade facilitates *Salmonella* survival by evading host antimicrobial peptide defence mechanisms. **(A)** *In vitro* polymyxin treatment survival assay of STM WT, STM *ΔluxS*, STM *ΔlsrB*, STM *ΔlsrK,* and STM *ΔlsrR*. Represented as Mean+/-SD of N=3, n=2. **(B)** mRNA expression of *pmrD*, *pmrA,* and *pmrB* in STM WT, STM *ΔluxS*, STM *ΔlsrB*, STM *ΔlsrK,* and STM *ΔlsrR* upon treatment of polymyxin in vitro LB media in mid-log phase culture (6h). Represented as Mean+/-SD of N=3, n=3. mRNA expression of **(C)** *pmrD*, **(D)** *pmrA* and **(E)** *pmrB* in STM WT, STM *ΔluxS*, STM *ΔlsrB*, STM *ΔlsrK,* and STM *ΔlsrR* upon infection in Caco-2 epithelial cells. Represented as Mean+/-SD of N=3, n=3. Two-way Anova was used to analyze the grouped data; p values **** $p < 0.0001$, *** $p < 0.001$, ** $p<0.01$, * $p<0.05$

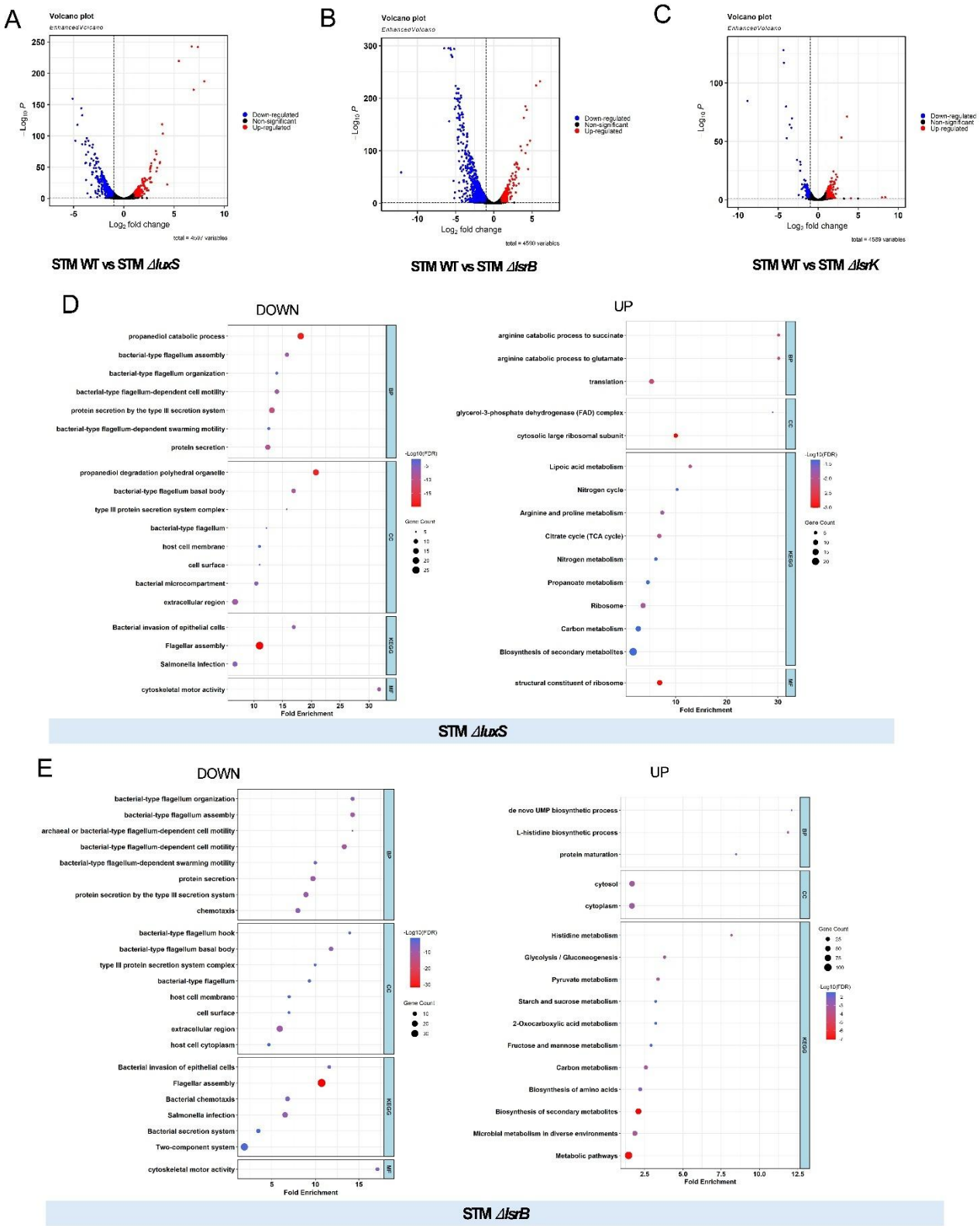
A
Volcano plot
EnhancedVolcano
Log10 P
Log2 fold change
Down-regulated
Non-significant
Up-regulated
STM WT vs STM ΔluxS
B
Volcano plot
EnhancedVolcano
Log10 P
Log2 fold change
Down-regulated
Non-significant
Up-regulated
STM WT vs STM ΔlsrB
C
Volcano plot
EnhancedVolcano
Log10 P
Log2 fold change
Down-regulated
Non-significant
Up-regulated
STM WT vs STM ΔlsrK
D
DOWN
propanediol catabolic process
bacterial-type flagellum assembly
bacterial-type flagellum organization
bacterial-type flagellum-dependent cell motility
protein secretion by the type III secretion system
bacterial-type flagellum-dependent swarming motility
protein secretion
propanediol degradation polyhedral organelle
bacterial-type flagellum basal body
type III protein secretion system complex
bacterial-type flagellum
host cell membrane
cell surface
bacterial microcompartment
extracellular region
Bacterial invasion of epithelial cells
Flagellar assembly
Salmonella infection
cytoskeletal motor activity
BP
CC
KEGG
MF
Fold Enrichment
UP
arginine catabolic process to succinate
arginine catabolic process to glutamate
translation
glycerol-3-phosphate dehydrogenase (FAD) complex
cytosolic large ribosomal subunit
Lipoic acid metabolism
Nitrogen cycle
Arginine and proline metabolism
Citrate cycle (TCA cycle)
Nitrogen metabolism
Propanoate metabolism
Ribosome
Carbon metabolism
Biosynthesis of secondary metabolites
structural constituent of ribosome
Fold Enrichment
STM ΔluxS
E
DOWN
bacterial-type flagellum organization
bacterial-type flagellum assembly
archaeal or bacterial-type flagellum-dependent cell motility
bacterial-type flagellum-dependent cell motility
bacterial-type flagellum-dependent swarming motility
protein secretion
protein secretion by the type III secretion system
chemotaxis
bacterial-type flagellum hook
bacterial-type flagellum basal body
type III protein secretion system complex
bacterial-type flagellum
host cell membrane
cell surface
extracellular region
host cell cytoplasm
Bacterial invasion of epithelial cells
Flagellar assembly
Bacterial chemotaxis
Salmonella infection
Bacterial secretion system
Two-component system
cytoskeletal motor activity
BP
CC
KEGG
MF
Fold Enrichment
UP
de novo UMP biosynthetic process
L-histidine biosynthetic process
protein maturation
cytosol
cytoplasm
Histidine metabolism
Glycolysis / Gluconeogenesis
Pyruvate metabolism
Starch and sucrose metabolism
2-Oxocarboxylic acid metabolism
Fructose and mannose metabolism
Carbon metabolism
Biosynthesis of amino acids
Biosynthesis of secondary metabolites
Microbial metabolism in diverse environments
Metabolic pathways
Fold Enrichment
STM ΔlsrB

780 **Fig. 6 LuxS/AI-2 signaling regulates critical gene targets to assist in multiple**
781 **stages of *Salmonella* infection in the host.** Transcriptomic analysis of STM WT,
782 STM *ΔluxS*, STM *ΔlsrB*, and STM *ΔlsrK* grown in LB media **(A-C)**. Gene
783 enrichment (GO) and KEGG analysis in STM *ΔluxS* and STM *ΔlsrB* **(D-E).**
784

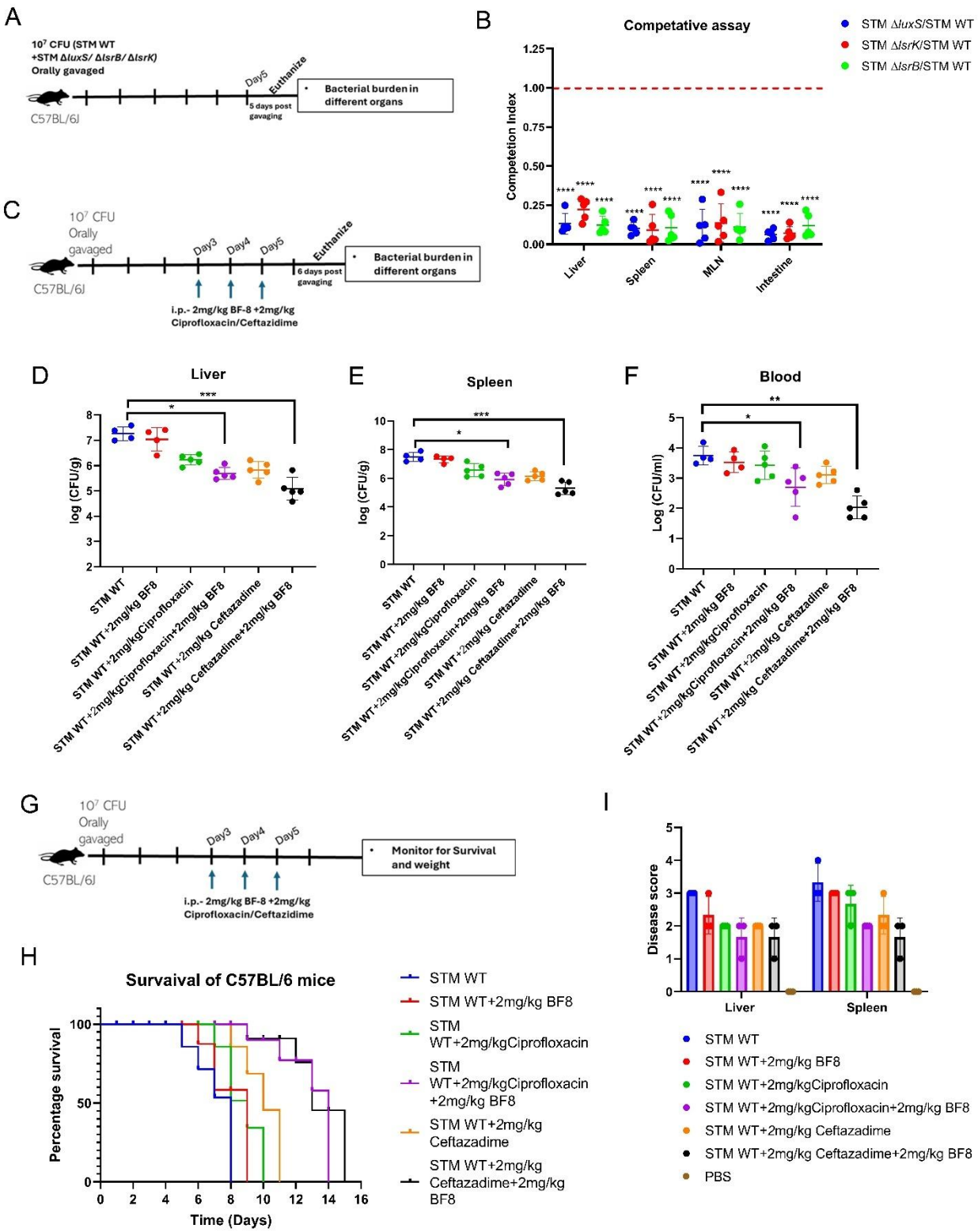

Fig. 7 Inhibition of LuxS/AI-2 signaling with antibiotics reduces *Salmonella* colonization *in vivo* and enhances mice survival. (A) The Competitive

789 experimental protocol for organ burden in C57BL/6J mice by orally gavaging a
790 total of 10^7 CFU per mouse. **(B)**The organ burden post 5 days of oral gavage in a
791 competition assay. Represented as Mean+/-SD of N=2, n=5 **(C)**. The
792 experimental protocol for C57BL/6J mice infected with STM WT by orally
793 gavaging 10^7 and BF-8 and an antibiotic treatment. Organ burden post treatment
794 **(D)** Liver, (**E)** Spleen, and **(F)** Blood. Represented as Mean+/-SD of N=2, n=5.
795 **(G)** The experimental protocol of mouse survival in C57BL/6J mice involved
796 orally gavaging 10^7 CFU per mouse upon treatment with the BF-8 inhibitor and
797 a combination of antibiotics (through the Intraperitoneal route). **(H)** Percentage
798 survival of Mice upon infection with STM WT with and without treatment. **(I)**
799 Disease score from the histopathological sections of the liver and spleen. Non-
800 parametric One-way ANOVA (Kruskal-Wallis) with Dunn's post hoc test was
801 used to analyze organ burden in mice.
802
803

References -

1. Nealson KH, Platt T, Hastings JW. Cellular control of the synthesis and activity of the bacterial luminescent system. Journal of bacteriology. 1970;104(1):313-22.
2. Fuqua WC, Winans SC, Greenberg EP. Quorum sensing in bacteria: the LuxR-LuxI family of cell density-responsive transcriptional regulators. Journal of bacteriology. 1994;176(2):269-75.
3. Bassler BL, Wright M, Showalter RE, Silverman MR. Intercellular signalling in Vibrio harveyi: sequence and function of genes regulating expression of luminescence. Molecular microbiology. 1993;9(4):773-86.
4. Taga ME, Bassler BL. Chemical communication among bacteria. Proceedings of the National Academy of Sciences. 2003;100(suppl_2):14549-54.
5. Asad S, Opal SM. Bench-to-bedside review: quorum sensing and the role of cell-to-cell communication during invasive bacterial infection. Critical care. 2008;12(6):236.
6. Greenberg EP. Bacterial communication and group behavior. The Journal of clinical investigation. 2003;112(9):1288-90.
7. Miller MB, Bassler BL. Quorum sensing in bacteria. Annual Reviews in Microbiology. 2001;55(1):165-99.
8. Ikuta KS, Swetschinski LR, Aguilar GR, Sharara F, Mestrovic T, Gray AP, et al. Global mortality associated with 33 bacterial pathogens in 2019: a systematic analysis for the Global Burden of Disease Study 2019. The Lancet. 2022;400(10369):2221-48.
9. Hajra D, Nair AV, Chakravortty D. Decoding the invasive nature of a tropical pathogen of concern: The invasive non-Typhoidal Salmonella strains causing host-restricted extraintestinal infections worldwide. Microbiological Research. 2023;277:127488.
10. Marcus SL, Brumell JH, Pfeifer CG, Finlay BB. Salmonella pathogenicity islands: big virulence in small packages. Microbes and infection. 2000;2(2):145-56.
11. Pradhan D, Devi Negi V. Stress-induced adaptations in Salmonella: A ground for shaping its pathogenesis. Microbiol Res. 2019;229:126311.
12. Gal-Mor O. Persistent Infection and Long-Term Carriage of Typhoidal and Nontyphoidal Salmonellae. Clin Microbiol Rev. 2019;32(1).
13. Fabrega A, Vila J. Salmonella enterica serovar Typhimurium skills to succeed in the host: virulence and regulation. Clin Microbiol Rev. 2013;26(2):308-41.
14. Miller MB, Bassler BL. Quorum sensing in bacteria. Annu Rev Microbiol. 2001;55:165-99.
15. Walters M, Sperandio V. Quorum sensing in Escherichia coli and Salmonella. Int J Med Microbiol. 2006;296(2-3):125-31.
16. Sholpan A, Lamas A, Cepeda A, Franco CM. Salmonella spp. quorum sensing: an overview from environmental persistence to host cell invasion. AIMS Microbiol. 2021;7(2):238-56.
17. Rezzonico F, Smits TH, Duffy B. Detection of AI-2 receptors in genomes of Enterobacteriaceae suggests a role of type-2 quorum sensing in closed ecosystems. Sensors (Basel). 2012;12(5):6645-65.
18. Miller ST, Xavier KB, Campagna SR, Taga ME, Semmelhack MF, Bassler BL, et al. Salmonella typhimurium recognizes a chemically distinct form of the bacterial quorum-sensing signal AI-2. Mol Cell. 2004;15(5):677-87.
19. Vendeville A, Winzer K, Heurlier K, Tang CM, Hardie KR. Making 'sense' of metabolism: autoinducer-2, LuxS and pathogenic bacteria. Nat Rev Microbiol. 2005;3(5):383-96.
20. Chatterjee R, Shreenivas MM, Sunil R, Chakravortty D. Enteropathogens: Tuning Their Gene Expression for Hassle-Free Survival. Frontiers in microbiology. 2018;9:3303.
21. Choi J, Shin D, Kim M, Park J, Lim S, Ryu S. LsrR-mediated quorum sensing controls invasiveness of Salmonella typhimurium by regulating SPI-1 and flagella genes. PloS one. 2012;7(5):e37059.

22. Choi J, Park J, Ryu S. Repressed Quorum sensing by overexpressing LsrR Hampers Salmonella evasion from oxidative killing within macrophages. Journal of microbiology and biotechnology. 2010;20(12):1624-9.
23. Wang Y, Liu B, Grenier D, Yi L. Regulatory Mechanisms of the LuxS/AI-2 System and Bacterial Resistance. Antimicrobial agents and chemotherapy. 2019;63(10).
24. Laganenka L, Colin R, Sourjik V. Chemotaxis towards autoinducer 2 mediates autoaggregation in Escherichia coli. Nat Commun. 2016;7:12984.
25. Laganenka L, Lee JW, Malfertheiner L, Dieterich CL, Fuchs L, Piel J, et al. Chemotaxis and autoinducer-2 signalling mediate colonization and contribute to co-existence of Escherichia coli strains in the murine gut. Nat Microbiol. 2023;8(2):204-17.
26. Ismail AS, Valastyan JS, Bassler BL. A Host-Produced Autoinducer-2 Mimic Activates Bacterial Quorum Sensing. Cell Host Microbe. 2016;19(4):470-80.
27. Hegde M, Englert DL, Schrock S, Cohn WB, Vogt C, Wood TK, et al. Chemotaxis to the quorum-sensing signal AI-2 requires the Tsr chemoreceptor and the periplasmic LsrB AI-2-binding protein. Journal of bacteriology. 2011;193(3):768-73.
28. Rodrigues MV, Ferreira A, Ramirez-Montoya M, Oliveira RA, Defaix R, Kis P, et al. Manipulation and quantification of the levels of Autoinducer-2 quorum sensing signal in the mouse gut. Bioorg Chem. 2025;157:108274.
29. Datsenko KA, Wanner BL. One-step inactivation of chromosomal genes in Escherichia coli K-12 using PCR products. Proceedings of the National Academy of Sciences of the United States of America. 2000;97(12):6640-5.
30. Janssens JC, Steenackers H, Robijns S, Gellens E, Levin J, Zhao H, et al. Brominated furanones inhibit biofilm formation by Salmonella enterica serovar Typhimurium. Appl Environ Microbiol. 2008;74(21):6639-48.
31. Pan J, Bahar AA, Syed H, Ren D. Reverting antibiotic tolerance of Pseudomonas aeruginosa PAO1 persister cells by (Z)-4-bromo-5-(bromomethylene)-3-methylfuran-2(5H)-one. PloS one. 2012;7(9):e45778.
32. Simon Andrews F, Segonds-Pichon A, Biggins L, Krueger C, Wingett S. FastQC: a quality control tool for high throughput sequence data. 2010.
33. Chen S. Ultrafast one-pass FASTQ data preprocessing, quality control, and deduplication using fastp. Imeta. 2023;2(2):e107.
34. Kopylova E, Noé L, Touzet H. SortMeRNA: fast and accurate filtering of ribosomal RNAs in metatranscriptomic data. Bioinformatics. 2012;28(24):3211-7.
35. Kim D, Paggi JM, Park C, Bennett C, Salzberg SL. Graph-based genome alignment and genotyping with HISAT2 and HISAT-genotype. Nature biotechnology. 2019;37(8):907-15.
36. Liao Y, Smyth GK, Shi W. featureCounts: an efficient general purpose program for assigning sequence reads to genomic features. Bioinformatics. 2014;30(7):923-30.
37. Love MI, Huber W, Anders S. Moderated estimation of fold change and dispersion for RNA-seq data with DESeq2. Genome biology. 2014;15(12):550.
38. Garai P, Lahiri A, Ghosh D, Chatterjee J, Chakravortty D. Peptide utilizing carbon starvation gene yjiY is required for flagella mediated infection caused by Salmonella. Microbiology. 2016;162(1):100-16.
39. Nair AV, Singh A, Devasurmutt Y, Rahman SA, Tatu US, Chakravortty D. Spermidine constitutes a key determinant of Motility and attachment of Salmonella Typhimurium through a novel regulatory mechanism. Microbiol Res. 2024;281:127605.
40. Toker AS, Macnab RM. Distinct regions of bacterial flagellar switch protein FliM interact with FliG, FliN and CheY. J Mol Biol. 1997;273(3):623-34.
41. Sarkar MK, Paul K, Blair D. Chemotaxis signaling protein CheY binds to the rotor protein FliN to control the direction of flagellar rotation in Escherichia coli. Proceedings of the National Academy of Sciences of the United States of America. 2010;107(20):9370-5.

42. Aizawa S-I, Minamino T. Flagella. Molecular medical microbiology: Elsevier; 2024. p. 97-126.
43. Frye J, Karlinsey JE, Felise HR, Marzolf B, Dowidar N, McClelland M, et al. Identification of new flagellar genes of Salmonella enterica serovar Typhimurium. Journal of bacteriology. 2006;188(6):2233-43.
44. Mukherjee S, Bassler BL. Bacterial quorum sensing in complex and dynamically changing environments. Nat Rev Microbiol. 2019;17(6):371-82.
45. Kim MK, Ingremeau F, Zhao A, Bassler BL, Stone HA. Local and global consequences of flow on bacterial quorum sensing. Nat Microbiol. 2016;1:15005.
46. Millet YA, Alvarez D, Ringgaard S, von Andrian UH, Davis BM, Waldor MK. Insights into Vibrio cholerae intestinal colonization from monitoring fluorescently labeled bacteria. PLoS pathogens. 2014;10(10):e1004405.
47. Zhao X, Koestler BJ, Waters CM, Hammer BK. Post-transcriptional activation of a diguanylate cyclase by quorum sensing small RNAs promotes biofilm formation in Vibrio cholerae. Mol Microbiol. 2013;89(5):989-1002.
48. Carter PB, Collins FM. The route of enteric infection in normal mice. The Journal of experimental medicine. 1974;139(5):1189-203.
49. Niemann HH, Schubert WD, Heinz DW. Adhesins and invasins of pathogenic bacteria: a structural view. Microbes and infection. 2004;6(1):101-12.
50. Pizarro-Cerda J, Cossart P. Bacterial adhesion and entry into host cells. Cell. 2006;124(4):715-27.
51. Cooper KG, Kari L, Chong A, Tandon N, Doran K, Gomes Da Silva L, et al. HilD-regulated chemotaxis proteins contribute to Salmonella Typhimurium colonization in the gut. mBio. 2025;16(4):e0039025.
52. Cooper KG, Chong A, Kari L, Jeffrey B, Starr T, Martens C, et al. Regulatory protein HilD stimulates Salmonella Typhimurium invasiveness by promoting smooth swimming via the methyl-accepting chemotaxis protein McpC. Nat Commun. 2021;12(1):348.
53. Muniz LR, Knosp C, Yeretssian G. Intestinal antimicrobial peptides during homeostasis, infection, and disease. Frontiers in immunology. 2012;3:310.
54. Singh A, Nair AV, Aroli S, Das S, Karmakar S, Mukherjee S, et al. LuxS/AI-2 signaling in Salmonella Typhimurium regulates phoP/phoQ to protect against acidic pH for enhanced survival in macrophages. bioRxiv. 2025:2025.03. 26.645541.
55. Gunn JS, Miller SI. PhoP-PhoQ activates transcription of pmrAB, encoding a two-component regulatory system involved in Salmonella typhimurium antimicrobial peptide resistance. Journal of bacteriology. 1996;178(23):6857-64.
56. Shprung T, Peleg A, Rosenfeld Y, Trieu-Cuot P, Shai Y. Effect of PhoP-PhoQ activation by broad repertoire of antimicrobial peptides on bacterial resistance. The Journal of biological chemistry. 2012;287(7):4544-51.
57. Richards SM, Strandberg KL, Conroy M, Gunn JS. Cationic antimicrobial peptides serve as activation signals for the Salmonella Typhimurium PhoPQ and PmrAB regulons in vitro and in vivo. Front Cell Infect Microbiol. 2012;2:102.
58. Shprung T, Wani NA, Wilmes M, Mangoni ML, Bitler A, Shimoni E, et al. Opposing Effects of PhoPQ and PmrAB on the Properties of Salmonella enterica serovar Typhimurium: Implications on Resistance to Antimicrobial Peptides. Biochemistry. 2021;60(39):2943-55.
59. Shi Y, Latifi T, Cromie MJ, Groisman EA. Transcriptional control of the antimicrobial peptide resistance ugtL gene by the Salmonella PhoP and SlyA regulatory proteins. The Journal of biological chemistry. 2004;279(37):38618-25.
60. Chen HD, Jewett MW, Groisman EA. An allele of an ancestral transcription factor dependent on a horizontally acquired gene product. PLoS Genet. 2012;8(12):e1003060.

61. McPhee JB, Bains M, Winsor G, Lewenza S, Kwasnicka A, Brazas MD, et al. Contribution of the PhoP-PhoQ and PmrA-PmrB two-component regulatory systems to Mg2+-induced gene regulation in Pseudomonas aeruginosa. Journal of bacteriology. 2006;188(11):3995-4006.
62. Groisman EA. The pleiotropic two-component regulatory system PhoP-PhoQ. Journal of bacteriology. 2001;183(6):1835-42.
63. Galan JE. Salmonella Typhimurium and inflammation: a pathogen-centric affair. Nat Rev Microbiol. 2021;19(11):716-25.
64. Haraga A, Ohlson MB, Miller SI. Salmonellae interplay with host cells. Nat Rev Microbiol. 2008;6(1):53-66.
65. Nair AV, Singh A, Rajmani RS, Chakravortty D. Salmonella Typhimurium employs spermidine to exert protection against ROS-mediated cytotoxicity and rewires host polyamine metabolism to ameliorate its survival in macrophages. Redox Biol. 2024;72:103151.
66. Ha JH, Hauk P, Cho K, Eo Y, Ma X, Stephens K, et al. Evidence of link between quorum sensing and sugar metabolism in Escherichia coli revealed via cocrystal structures of LsrK and HPr. Science advances. 2018;4(6):eaar7063.
67. Oliveira RA, Cabral V, Torcato I, Xavier KB. Deciphering the quorum-sensing lexicon of the gut microbiota. Cell Host Microbe. 2023;31(4):500-12.
68. Thompson JA, Oliveira RA, Djukovic A, Ubeda C, Xavier KB. Manipulation of the quorum sensing signal AI-2 affects the antibiotic-treated gut microbiota. Cell reports. 2015;10(11):1861-71.
69. Lagkouvardos I, Lesker TR, Hitch TC, Gálvez EJ, Smit N, Neuhaus K, et al. Sequence and cultivation study of Muribaculaceae reveals novel species, host preference, and functional potential of this yet undescribed family. Microbiome. 2019;7:1-15.
70. Hegde M, Englert DL, Schrock S, Cohn WB, Vogt C, Wood TK, et al. Chemotaxis to the quorum-sensing signal AI-2 requires the Tsr chemoreceptor and the periplasmic LsrB AI-2-binding protein. Journal of bacteriology. 2011;193(3):768-73.
71. Shprung T, Peleg A, Rosenfeld Y, Trieu-Cuot P, Shai Y. Effect of PhoP-PhoQ activation by broad repertoire of antimicrobial peptides on bacterial resistance. Journal of Biological Chemistry. 2012;287(7):4544-51.
72. McPhee JB, Bains M, Winsor G, Lewenza S, Kwasnicka A, Brazas MD, et al. Contribution of the PhoP-PhoQ and PmrA-PmrB two-component regulatory systems to Mg2+-induced gene regulation in Pseudomonas aeruginosa. Journal of bacteriology. 2006;188(11):3995-4006.
73. Molloy MJ, Grainger JR, Bouladoux N, Hand TW, Koo LY, Naik S, et al. Intraluminal containment of commensal outgrowth in the gut during infection-induced dysbiosis. Cell Host Microbe. 2013;14(3):318-28.
74. Haag LM, Fischer A, Otto B, Plickert R, Kuhl AA, Gobel UB, et al. Intestinal microbiota shifts towards elevated commensal Escherichia coli loads abrogate colonization resistance against Campylobacter jejuni in mice. PloS one. 2012;7(5):e35988.